



Chair:
Prof. Paola Taroni

DOCTORAL PROGRAM IN PHYSICS

The Doctoral Program in Physics at Politecnico di Milano aims at attracting bright students with good scientific background and clear interest towards development and applications of new ideas and technologies. It offers a wide range of opportunities in the fields of advanced applied physics, such as photonics and optoelectronics (lasers, ultrafast optics), biomedical optics (optical tomography), vacuum technologies (thin film depositions), material technologies (microelectronics and nanotechnologies, micromechanical processing), and advanced instrumentation (electronic and atomic microscopy, nuclear magnetic resonance).

Scientific education and training to develop general research abilities in all areas of applied physics is increasingly needed by advanced technological companies. Through a general education in the basic areas of applied physics and a specific knowledge in condensed matter physics, as well as optics and lasers, the PhD Program aims at the development of an experimental approach to problem solving techniques and at the attainment of a high level of professional qualification.

The Doctoral Program has strongly experimental character. The contents are strictly related to the research activities carried out in the laboratories at the Department of Physics. They can be divided into two main areas:

- a) Condensed Matter Physics, including photoemission; spin-resolved electronic spectroscopy; magneto-optics; X ray diffraction; magnetic nanostructures for spintronics; synchrotron radiation spectroscopy, positron spectroscopy, semiconductor nanostructures.
- b) Photonics and Quantum Electronics, including ultrashort light pulse generation and applications; UV and X optical harmonics generation; biomedical applications of lasers; diagnostics for works of art; laser applications in optical communications; time domain optical spectroscopy and diagnostic techniques.

All research activities rely on advanced experimental laboratories located at Politecnico di Milano (Milano-Leonardo Campus and Como Campus) and are performed in collaboration with several international Institutions. Consistent effort is devoted to experimental research, development of innovative approaches and techniques, and design of novel instrumentation.

The educational program can be divided into three parts: 1) Main courses specifically designed for the PhD program; 3) Activities pertaining to more

specific disciplines which will lay the foundation for the research work to be carried out during the Doctoral Thesis; 4) Doctoral Thesis. The thesis work is the major activity of the Program. It has a marked experimental character, and will be carried out in one or more laboratories at the Department of Physics.

The students are also encouraged to perform part of their thesis work in laboratories of other national or foreign Institutions. Collaborations that may involve the PhD students are presently active with several national and international research and academic Institutions, such as: ETH-Zürich, EPL-Lausanne, Lund Institute of Technology, University of Paris-Sud, Ecole Polytechnique-Paris, University of Berkeley, University of Cambridge, University College London, Massachusetts Institute of Technology, Harvard University, European Space Agency, ENEA, Elettra-Ts, PSI-Villigen, Agenzia Spaziale Italiana, European Synchrotron Radiation Facility (ESRF-Grenoble), INFN-CNR, IIT-Istituto Italiano di Tecnologia.

The average number of fellowships available for students admitted to the PhD Program is fifteen per year. At present, the number of students in the three-year course is fifty-eight, and forty-seven of them have a fellowship.

The PhD Program Faculty, who takes care of organizing and supervising teaching and research activities, consists of a number of members large enough to cover a wide spectrum of research fields. All members (listed here below) are highly qualified and active researchers. This ensures a continuous updating of the PhD Program and guarantees that the students are involved in innovative research work.

The Doctoral Program relies also on the advice of a Steering Committee, formed by distinguished experts (see table below) coming from R&D industries or research laboratories, who take care that the goals of the PhD Program are in line with the needs of non academic world.

| FAMILY NAME | FIRST NAME | POSITION* |
|--------------|------------|-----------|
| BERTACCO | RICCARDO | AP |
| BRAMBILLA | ALBERTO | AP |
| CICCACCI | FRANCO | FP |
| CUBEDDU | RINALDO | FP |
| DALLERA | CLAUDIA | AP |
| D'ANDREA | COSIMO | AP |
| DELLA VALLE | GIUSEPPE | AP |
| DE SILVESTRI | SANDRO | FP |
| DUÒ | LAMBERTO | FP |
| FINAZZI | MARCO | AP |
| GHIRINGHELLI | GIACOMO | AP |
| ISELLA | GIOVANNI | AP |
| LANZANI | GUGLIELMO | FP |
| LAPORTA | PAOLO | FP |
| MARANGONI | MARCO | AP |
| NISOLI | MAURO | FP |
| RAMPONI | ROBERTA | FP |
| STAGIRA | SALVATORE | AP |
| TARONI | PAOLA | FP |
| TORRICELLI | ALESSANDRO | AP |

*Position: FP = Full Professor; AP = Associate Professor.

| FAMILY NAME | FIRST NAME | INSTITUTION |
|-------------|------------|------------------------------------|
| PIROVANO | AGOSTINO | Micron Semiconductor Italia s.r.l. |
| DONATI | FABIO | EPFL - Lausanne, CH |
| MIOZZO | LUCIANO | Solvay Specialty Polymers |
| von KÄENEL | HANS | ETH - Zürich, CH |
| MASOTTI | GIOVANNI | El.En. S.p.A |

LINEAR AND NONLINEAR OPTICAL PROPERTIES OF PLASMONIC NANOANTENNAS

Milena Baselli - Supervisor: Marco Finazzi

Antennas allow to produce electromagnetic waves with a well defined radiation pattern, in order to send signals or power over large distances. Moreover, they are able to receive electromagnetic waves from remote sources. One of the feature that make antennas essential in the technological scenario is their ability to connect information processing using electrical signals and wireless transmission of information. The operating principle of these devices is based on the oscillation of charges inside their volume. When an e.m.wave reaches the antenna or an ac voltage is applied the charges are constricted to move in a well defined regions of space. This motion affect the electric field at any distance from the source through the creation of e.m. disturbances. The simplest antenna that one can think about can be realized connecting two metallic spheres with a thin wire. When the system is prepared in an initial state with the two spheres charged with opposite signs, the charges will start to oscillate at a frequency $\omega_0 = 1/\sqrt{LC}$ where L indicates the inductance and C the capacitance. Antennas of every possible shape can be characterized by these two parameters. Changing the

geometrical parameters they can be tuned, in order to tune the frequency in the desired regime. Moving to the infrared and visible part of the spectrum, metals no longer behave as perfect conductors and Ohmic losses can't be neglected anymore. Nanoparticles that are made of certain materials (for example gold or silver) display resonances in these regime. These phenomena are called localized surface plasmon resonances (LSPR) and can be exploited in order to balance drawbacks due to the losses. The scientific community has identified this special nanoparticles, called plasmonic nanoparticles, as the best candidates for the implementation of antennas working at the NIR/VIS wavelengths. One important feature of the LSPR is the ability to enhance the electric field in regions immediately close to the particle surface. Therefore plasmonic antennas provide an important interface between quantum emitters and the far field. Another important characteristic of plasmonic resonances is their extreme sensitivity to changes in the refractive index of the media surrounding the particle. For this reason, conveniently functionalized plasmonic

antennas has been identified as an interesting basis for new generation biosensors. Moreover it has been shown that arrays of antennas can be used to compose surfaces with particular optical properties, called "metasurfaces". The antennas that constitute these particular optical components are designed in order to have a precise phase lag one with respect to the others in the complex polarizability. In the first part of this thesis a method to retrieve the complex polarizability is applied to gold gap antennas. This procedure have been previously applied successfully to spherical nanoparticles and nanorods. The optical contrast observed in near-field microscopy of gold nanoparticles is ruled by the interference between the field emitted by the tip and the one radiated by the plasma oscillations in the nanoparticle. Such interference generates a positive (negative) contrast for particles illuminated below (above) resonance, a behavior ruled by the phase of the particle complex polarizability. By combining far-field confocal extinction microscopy with SNOM imaging employing hollow-pyramid probes, it is possible to disentangle the real and imaginary part of

the particle polarizability. By comparing near-and far-field optical microscopy performed on an array of antennas with varying arm lengths, we observe a reversal of the sign of the near-field contrast occurring at shorter antenna length with respect to the one resonating at the illumination wavelength, at variance with what we found on nanorods, where the contrast sign reversal occurs at resonance. Finite-difference time-domain simulations and an analytical model provide a rationale explaining this observation in terms of a non negligible influence of ohmic losses in defining the near field contrast of gap antennas. In the second part of this manuscript plasmonic nanoantennas for biosensing applications have been studied. Plasmonic biosensors are already on the market in the planar surface plasmon resonance configuration. Such devices have intrinsic limits in sensitivity and miniaturization. Moreover, they require to be supplied with a thermal stabilization. In order to overcome these drawbacks the scientific community are currently designing and testing plasmonic sensing devices based on nanoparticles. These are grown on the top of transparent substrates and properly functionalized in order to selectively bind a specific analyte. When the analyte reacts with the surface of the particles, the LSPR wavelength changes because of the changing in the refractive index. The analytes in solution can be delivered through microfluidic channels

and the LSPR wavelength is tracked through scattering experiment in transmission configuration. My coworkers and me decided to apply the second harmonic generation technique to this kind of biosensors. Our goal was to build a nanoparticle based sensor, monitoring the second harmonic signal generated instead of the linear one. Second harmonic generation (SHG) is a powerful imaging tool that allows background free investigations. Plasmonic materials have a centrosymmetric crystalline structure therefore the second harmonic generation process is inhibited from the bulk. Since the whole signal is generated from the surface, second harmonic generation is extremely sensitive to the change in the refractive index and can be fruitfully exploited for biosensing purpose. In order to obtain dipole allowed SHG the antennas must be shaped in a broken symmetry geometry. In 2015 we demonstrated a nano device for enhanced SHG. The operating principle is based on a multiresonant response at both the excitation and SH wavelength. The geometrical parameters are tuned in order to place two plasmonic modes exactly at the fundamental and at the SH frequency. This feature allows to increase the absorption and the scattering of the nonlinear signal. Moreover, due to the special design, a significant spatial overlap of the localized fields at the wavelengths of interest occurs. According to our experiments, the double resonant antenna displayed a second

harmonic generation efficiency $\beta_{SH} = P_{SH}/P_{FW}^2 \approx 5 \times 10^{-5}$. We estimated that this value is between one and two orders of magnitude larger than the values reported in literature for similar structures. The small gap required the use of focus ion beam milling technique for the fabrication. Although almost perfect structures can be obtained with this procedure, the large costs and time required inhibited its application to commercial devices. In order to overcome these drawbacks, we performed further studies and experiments on a geometry that can be easily obtained with electron beam lithography. We explored a matrix of L shaped antennas periodically spaced, placed on a glass substrate. Performing computational simulation with the software Reticolo (Matlab) we optimized the geometrical parameters. We found that with this kind of geometry it's not possible to place the plasmonic modes exactly at the frequencies of interest. Nevertheless, with the best parameters the absorption and scattering efficiencies at the FW and SH wavelengths respectively turned out to be adequately high. A sample has been fabricated with EBL by means of the well known lift off technique. The linear and nonlinear characterization revealed the FW absorption process to be much more significant than the SH scattering process in the overall SHG efficiency.

HYBRID INTERFACES BETWEEN CONJUGATED POLYMERS THIN FILMS AND AQUEOUS SOLUTIONS FOR ENERGETIC AND BIOLOGICAL APPLICATIONS

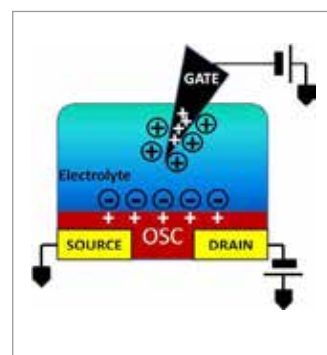
Sebastiano Bellani - Tutor: Prof. Guglielmo Lanzani
Supervisor: Dr. Maria Rosa Antognazza

In recent years, research on conjugated polymers started to advance its frontiers beyond the applications in light emitting diodes, photovoltaic cells and transistors, facing new challenges in the fields of photoelectrochemistry and biology. A plethora of novel possible applications of organic semiconductors (OSCs) have been reported, including organic photoelectrochemical cells (OPECs), organic field effect transistors (OFETs) for elicitation and recording of cellular activity, water-gated organic field effect transistors (WGOFETs) for bio and environmental sensing, and photo-active interfaces with living cells and tissues. The common denominator of all these proof-of-concept devices is the direct contact between the active polymer surface and a liquid component, which in most cases is an aqueous solution. The aim of this work is to provide a detailed chemical-physical, spectroscopic, optoelectronic and electrochemical characterization of different polymer/liquid hybrid interfaces. First, we report a comprehensive study of chemical-physical effects occurring in thin films of regioregular poly(3-hexylthiophene) (rr-P3HT),

the election material for such applications, exposed to different environmental conditions. In particular, its contact with water and possible relative changes in materials is deeply studied with optical spectroscopy methods, allowing to establish that the bulk optoelectronic properties of OSCs are not seriously affected. In addition, sum-frequency generation vibrational spectroscopy, a surface-specific technique compatible with electrochemical/biological conditions, demonstrates that the surface of thin films rr-P3HT undergoes a molecular reorientation when exposed to aqueous electrolytes, with respect to their surface structure in air. Continuous wave photo-induced absorption measurements reveals that the charge photogeneration for the rr-P3HT when blended with a typical donor component, i.e. [6,6]-phenyl-C₆₁-butyric acid methyl ester (PCBM), is preserved in both aqueous and acetonitrile-based solutions. Moreover, we present a thorough electrochemical characterization of different hybrid polymer/electrolyte interfaces, focusing on capacitive and faradaic processes occurring at the polymer surface upon illumination and/or

applying an external bias. Based on this knowledge, we explore organic semiconducting materials in two different fields.

- i) Biological applications. The possibility to use P3HT films as artificial photoreceptor layers, capable to restore light sensitivity in blind retinas, was recently reported by our group. The acquired knowledge of the polymer/electrolyte interface represents the necessary starting point for the complete understanding of the main mechanisms occurring at the interface between the conducting polymer and the living cells/tissues, and for their further exploitation in implantable devices. In addition, we develop

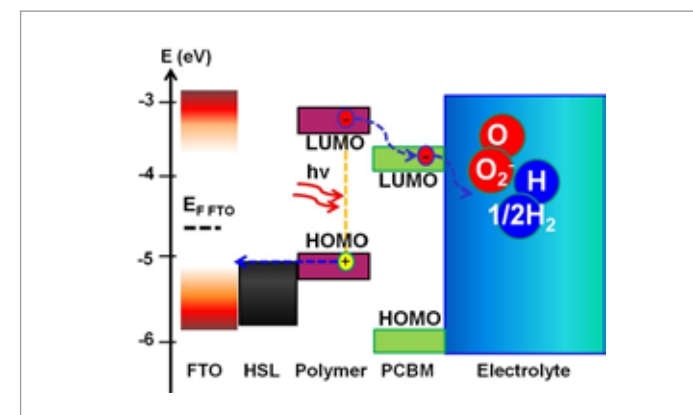


1. Schematic structure of a WGOFET device

different architectures of WGOFETs, which are playing an increasingly important role as sensors for biomedical and environmental applications (Figure 1)

By employing different polythiophene derivatives as *p*-type materials we highlight the specific role played by the double-layer capacitance at the semiconductor-electrolyte interfaces, as determined by a specific orientation of the polymer alkyl-side chains at the interface with water. In addition, we report the first demonstration of three working *n*-type WGOFETs, based on different materials, namely bithiophene-naphthalene diimide copolymer (PNDIT2), selenophene-vinylene-selenophene-naphthalene diimide copolymer (PNDISVS) and PCBM. The opportunity to employ *n*-type materials will certainly open up new perspectives in organic bioelectronics devices.

- ii) Energetic applications. We establish conjugated polymers as a promising class of materials for OPECs for sensing applications



2. Schematic representation of an OPEC.

and fuel cells. In particular we demonstrate the possibility to use OSCs to develop a highly sensitive photoelectrochemical dissolved oxygen (DO) sensor as well as efficient hybrid organic-inorganic photocathodes for aqueous H₂ production (Figure 2). Our findings suggest paths for future developments, offering a new lever for the sustainable and low-cost H₂ production.

ORGANIC THERMOELECTRICS FOR HUMAN BODY ENERGY HARVESTING

Davide Beretta - Supervisor: Prof. Guglielmo Lanzani

The thermoelectric effects consist in the conversion between thermal and electrical energy. When properly engineered, they allow for thermal energy into electricity conversion, and for precise climate conditioning. A typical thermoelectric device is made by many thermocouples (p-n couples), connected electrically in series and forming a thermal parallel, and sandwiched between two electrically insulating layers. Applying a temperature gradient between the insulating layers, a current is generated, and the device work as a thermoelectric generator (TEG). On the contrary, when a current is forced into the device, heat and/or cooling of the junctions due to the Peltier effect provides environmental thermal conditioning. The conversion efficiency of such devices, is as high as the thermocouple figure of merit, where α and σ are the electrical resistance series and the thermal conductance parallel of the constituent thermocouples, and κ is their thermopower squared. In order to compare the thermoelectric attitude of single materials, the material figure of merit has been introduced, where α is the thermopower, σ and κ the electrical and thermal

conductivity respectively. The higher is the figure of merit, the higher is the thermoelectric capacity of the material. TEGs have been used so far only in niche applications, such as space missions, because of materials cost and toxicity. But with the progress made in the last 20 years, industrial and automotive applications have become a reality. Moreover, with the downscaling of the electronic devices, sensors and wifi systems demanding powers in the order of 100 μ W, are now available. Micro generators for low power systems have been realized in order to provide small amount of power and thus represent an alternative to batteries and cables. In this framework, conducting polymers could provide a way to realize flexible micro-generators at low cost, thus allowing for human body energy harvesting in disposable applications. My graduate work on Organic thermoelectrics for human body energy harvesting has been the first one on the topic at CNST, thus giving me the opportunity to face many aspects of the research on thermoelectrics. Everything started with the laboratory set up. I spent more than one year designing and realizing a highly reliable system for the

simultaneous measurement of the thermopower and the electrical conductivity under vacuum, acquiring a strong knowledge in the field of vacuum systems technology and electrical and thermal characterization. This first work culminate in a publication for RSI in which, finally, accurate and precise Seebeck coefficient measurement of organic materials has also been demonstrated. Subsequently, the system has been intensively used to characterize organic and inorganic samples. Special attention has been given to polymeric (semi)conductors to investigate the validity of the Mott's relation in such systems and thus to identify some guidelines for thermoelectric improvements in organic matter. Informations from UPS, thermopower, electrical conductivity, and attempt of mobility, measurements, have been used to determine the degeneracy of those materials, and recognize the strong influence of the mobility on the charge carrier energy, asking for deeper investigation of their bulk mobility. Still, we agree with other authors that moving towards semi-metals could be a successful route to improve thermoelectric properties even

in organic matter. In parallel, my research focused on the design and fabrication of the first flexible, vertical, micro organic thermoelectric generator with high packing density of thermocouples. The power output of TEGs is maximum when the thermal resistance of the device matches the environment coupling one. Since this match cannot be achieved in generators made of short legs (such as micro-TEGs), and since the power output scales quadratically with the number of thermocouples, high packing density represents a good way to compensate for the thermal matching. Recently, many authors have demonstrated flexible generators, both organic and inorganic, but organic ones have been limited to planar architecture only. If the fabrication process of planar devices is relatively simple and definitely cheaper, planar geometries are not ideal for waste heat energy harvesting. Folding techniques to recover "vertical" architectures from planar structures have been proposed, but the resulting device is no more a micro generators, having a bulky structure, and therefore its flexibility is reduced. This poses a limit to the integration with

human bodies. For this reason, we moved towards vertical micr architectures. I developed a fabrication process on flexible substrates, involving thermal evaporation, photolithography and inkjet printing techniques, and I recently obtained a demonstrator of an organic TEG made of 8 thermocouples of p- and n-type polymers. The fabrication of a whole device made of many couples is on the way right now. Measuring the conversion efficiency and the power output of micro-TEGs is not easy. In particular, efficiency measurement is extremely complicated, since it involves the measurement of the absorbed heat flux. I have designed and realized another vacuum system, which can measure bulk and micro devices, and mounts a special device holder which allows for the characterization of flexible devices with different degrees of curvature. The system has been tested with commercial micro generators from MicroPelt, with results in good agreement with manufacturer specifications. The system is about to be updated to a more user friendly version, after which a publication will follow. In conclusion, we have set up a research line on thermoelectrics for room temperature

applications, especially focused on organic matter. Investigation techniques for successful studies have been identified, and reliable instrumentations for air sensitive materials and devices characterization, have been designed and realized. Some insights about the Mott's relation in conducting polymers have been exploited, and a demonstrator of a vertical thermoelectric generator has been given.

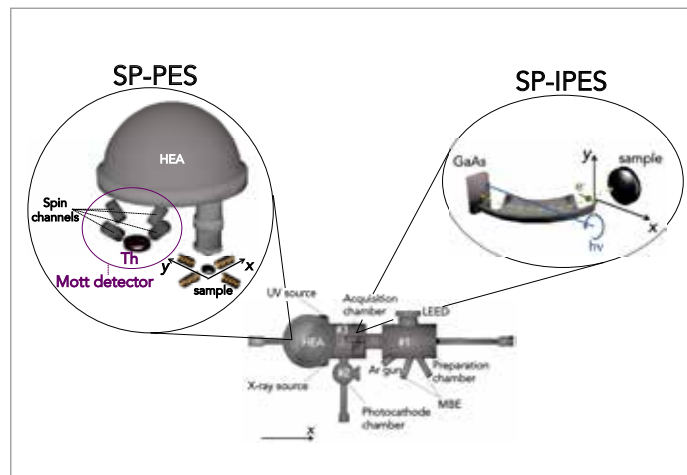
SPECTROSCOPIC INVESTIGATIONS OF FERROMAGNETIC SURFACES AND FERROMAGNET/ANTIFERROMAGNET INTERFACES

Giulia Berti - Supervisor: Prof. Alberto Brambilla

In spintronics (spin transport electronics or spin-based electronics) the information to be delivered is carried by the spin of the electrons instead of their charge. This gives the possibility to build a new generation of devices combining standard electronics with spin-dependent effects that arise from the interaction between the spin of the carrier and the magnetic properties of the material. In the general case, the use of the spin information is based on its alignment (either “up” or “down”) relative to a reference (an applied magnetic field or magnetization orientation of the ferromagnetic film). Device operations then rely on some quantity (electrical current) that depends, in a predictable way, on the degree of alignment. Adding the spin degree of freedom to conventional charge-based electronics or using the spin degree of freedom alone will add substantially more capability and performance to electronic products. The advantages of these new devices would be nonvolatility, increased data processing speed, decreased electric power consumption, and increased integration densities compared with conventional semiconductor technology. Among the candidate materials

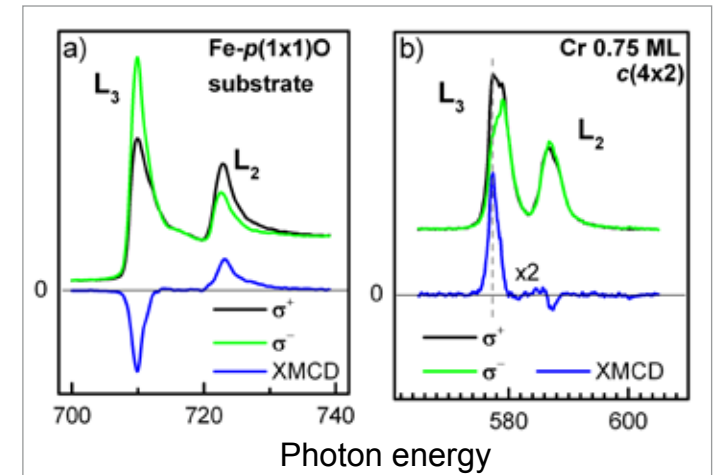
for the construction of this new-generation devices, there are transition metals and their oxides. They have been widely studied over the last decades because of the great interest in their basic physics and in the large range of applications they can be employed into. On the other hand, because of the tendency towards scaling of devices, one has to deal with present the drawback of surface and interface effects. Moreover, a severe limit to the miniaturization of such devices might come from the morphology and chemistry of the materials involved: in this

sense, the presence of atomically flat surfaces and sharp interfaces would pave the way towards real atomic-scale technology. My research activity has been dealing with the characterization of such systems by means of surface sensitive techniques. The experimental setup used in the laboratory is a ultra-high vacuum-based system (Fig.1) equipped with facilities for photoemission spectroscopy (for the study of occupied electron levels) and inverse photoemission spectroscopy (for the investigation of electronic states above the Fermi edge). The aforementioned setup was

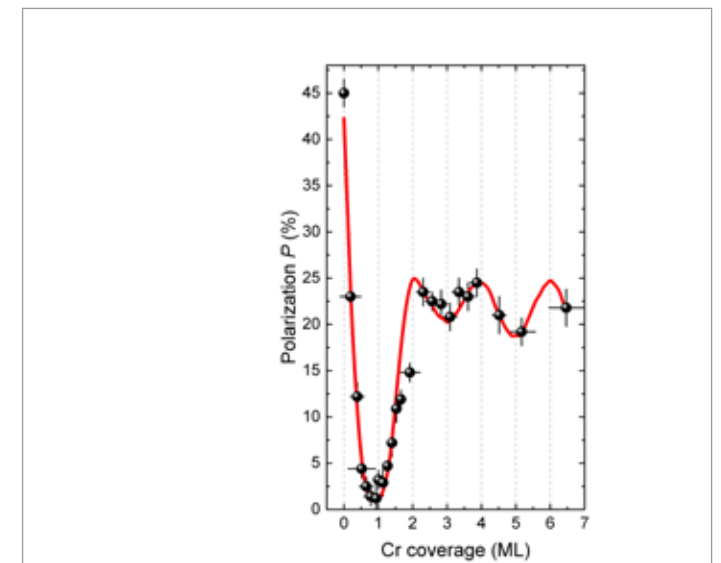


1. Sketch of the photoemission setup used for the spin-polarized analysis from both full (SP-PES) and empty (SP-IPES) electron states. The insets and the main picture are rotated with respect to each other as can be seen from (x,y) axes directions.

employed for the study of low-dimensional systems such as Ni/W, Ni/Fe, and Cr/Fe. Since the goal of my PhD activity was to study also the spin properties of the surfaces, I exploited the possibility of carrying out the analysis of both full and empty electron levels with the addition of spin polarization: in inverse photoemission this is achieved with a polarized electron source, while in standard photoemission the spin information comes from a spin detector (Mott detector) attached to the exit side of the hemispherical electron analyzer (see blow-ups in Fig. 1). Other experiments were performed at the beamline BACH of the Italian synchrotron Elettra, in Trieste, regarding the absorption of polarized X-rays. When the impinging photon beam is circularly polarized, indeed, the absorption probability of X-rays, which results in an electron transition towards a higher energy state, depends on the spin of the electron itself. If an imbalance in the spin populations exists near the Fermi edge, this can be probed by X-ray absorption. What gives the information about such an imbalance (i.e., information on the magnetic state of the sample) is the X-ray magnetic circular dichroism signal, XMCD, that is the result of the difference between two absorption spectra, namely acquired with positive and negative helicity of light, respectively. From such experiment, the alignment of Cr atoms moments on top of a ferromagnetic Fe(100) surface was analyzed, finding that the



2. XAS spectra at L_{2,3} edges for Fe (panel a) and Cr (panel b) taken with either positive (black lines) or negative (green lines) photon helicity, and XMCD signals (blue lines) of: panel (a) the Fe(100) substrate; panel (b) 0.75 ML of Cr on the Fe(100) substrate.



3. Polarization P at a binding energy of 1.6 eV, as a function of the Cr coverage. The line is a guide to the eye.

XMCD signal in the energy region of the Cr L_{2,3} edges had opposite sign with respect to that of the Fe substrate (see Fig. 2). Such result is in agreement with density functional theory calculations.

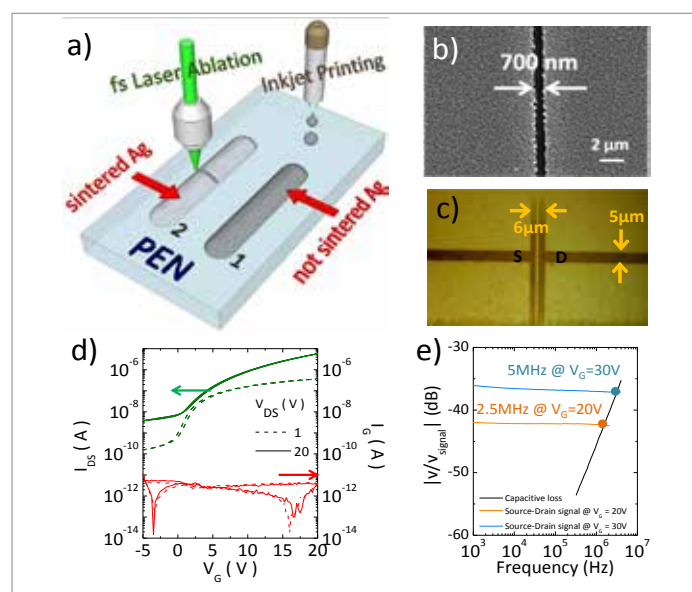
HIGH PERFORMANCE PRINTED ORGANIC AND HYBRID ELECTRONICS THROUGH SCALABLE TECHNIQUES

Sadir Gabriele Bucella - Supervisor: Prof. Guglielmo Lanzani

Solution processable high mobility semiconducting polymers and single walled carbon nanotubes (s-SWCNTs) offer a concrete opportunity to develop flexible and large area electronics. In the perspective of the industrial production, up-scalable large area deposition processes, such as the common graphical arts printing techniques, are widely investigated. However the limited resolutions ($>10\mu\text{m}$) are not compatible with microelectronics in which the performances would benefit from the miniaturization of the critical features. Moreover the tendency of materials from solution to form bulk film with high degree of disorder introduces high variability in the devices operation, a crucial aspect in the large scale fabrication, and the morphology control on large area is still a great challenge. In this Ph.D dissertation, the work is divided in three main parts: 1) the investigation of up-scalable direct writing processes for the fabrication of all solution processable organic FETs with submicron features on flexible substrates; 2) The printing of s-SWCNTs networks for high performance FETs; 3) the control of the assembling of a model naphthalene-diimide based polymeric semiconductor [P(NDI2OD-T2)] over large area by using a roll-to-roll bar

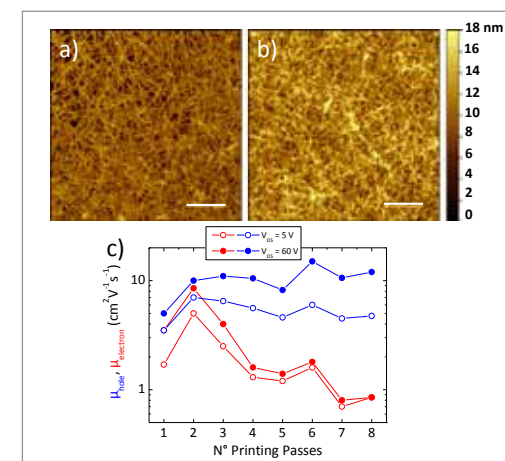
coating technique. In the first part, conducting lines, made of polymeric conductor (PEDOT:PSS) or silver, are deposited on flexible substrate through Drop-on-Demand inkjet printing methods. To overcome the resolution limit of the techniques ($\sim 30\mu\text{m}$), a femtosecond pulsed laser is adopted to pattern the conducting lines, obtaining two electrodes, source and drain, with lateral dimension down to

$3\mu\text{m}$, separated by a channel with a minimum length of approximately 700nm . The FETs are thus completed by inkjet printing the semiconducting layer (P(NDI2OD-T2)) and the gate electrode (PEDOT:PSS) and by spin-coating the organic dielectric layer (PMMA). The devices show mobility values above $0.1\text{cm}^2\text{V}^{-1}\text{s}^{-1}$ at a driving voltage of $V_G = 30\text{V}$ that, in combination with the small features produced, result in



1. a) Sketch of the direct writing process for the patterning of the source and drain electrodes. b) Scanning Electron Microscopy picture of a cut produced with fs-laser on a silver printed line. c) Picture of an inkjet printed PEDOT:PSS line after the patterning through the fs-laser. d) Transfer characteristic of a device obtained with the patterning in c). In red the leakage current through the insulator and in green the source and drain current. e) Frequency characterization of a device made with the source and drain of figure c).

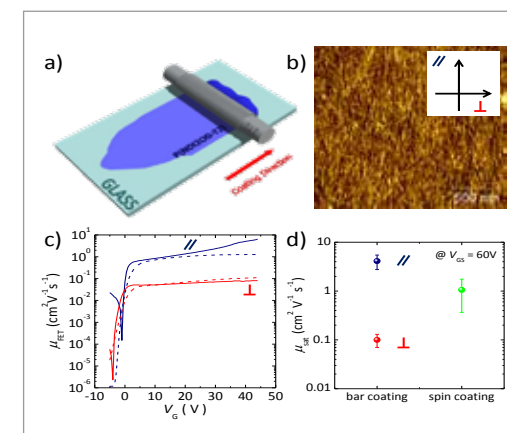
a maximum switching frequency of the devices of 5 MHz. The high yield of the process here described allows the integration of many working devices on the same substrate for the realization of complementary Inverters and Ring Oscillators. In the second part, inkjet printing is involved in the deposition of a semiconducting SWCNTs dispersion. Starting from a random population of HiPco nanotubes in powder, semiconducting chiralities are sorted in solution by a non covalent functionalization through P3DDT polymer chains. The P3DDT wrapped s-SWCNTs based dispersion is formulated so as to be compatible with the inkjet printing process. To fabricate the FETs, s-SWCNTs are printed directly on gold source and drain electrodes, pre-patterned by standard photolithography, resulting in a well-connected network. The dielectric layer (PMMA) is then



2. Atomic Force Microscopy maps of SWCNTs network obtained by a) a single printed pass and b) five printed passes. c) Mobility versus the increasing number of printing passes. The hole mobility (blue lines) and electron mobility (red lines) in linear regime (empty symbols) and saturation regime (filled symbols) are reported.

spun on the top and the gate electrodes is inkjet printed with PEDOT:PSS. By controlling the density of the network, varying the printing passes, FETs with ambipolar operation (hole mobility up to $10\text{cm}^2\text{V}^{-1}\text{s}^{-1}$ and electron mobility up to $7\text{cm}^2\text{V}^{-1}\text{s}^{-1}$) as well as unipolar p-type behavior (hole mobility up to $15\text{cm}^2\text{V}^{-1}\text{s}^{-1}$) are demonstrated. The tuning of the electronic properties through the simple control of the printing process allows the fabrication of a complementary-like inverter with the adoption of the same ink. In the third part, a bar coating technique, composed of a stainless steel rod wound with a metallic wire is studied for the large area deposition of functional materials. P(NDI2OD-T2) in solution is doctored off by the scanning of the bar, put directly in contact with the substrate surface. The directional flow induced in combination with the self assembling properties of

the polymer in pre-aggregating solvents enable the formation of fibrils-like nanostructures oriented along the coating direction. FETs are fabricated to probe the electrical properties of the semiconductor along and perpendicularly to the fibrils axis. The mobility measured in the two directions show a marked anisotropy with a preferential transport along the coating direction ($\mu_{\text{sat}} = 6.4\text{cm}^2\text{V}^{-1}\text{s}^{-1}$). In addition the uniform fibrils alignment on large area ($8\times 8\text{cm}$) reduces the relative standard deviation of the transistors measured (30%) with respect to the FETs realized by spin coating (60%), important for the large scale production of devices. By reducing the solution concentration, the same technique allows the formation of a polymeric sub-monolayer ($\sim 2.4\text{nm}$) with mobility up to $0.14\text{cm}^2\text{V}^{-1}\text{s}^{-1}$, the highest so far achieved for such film thickness.

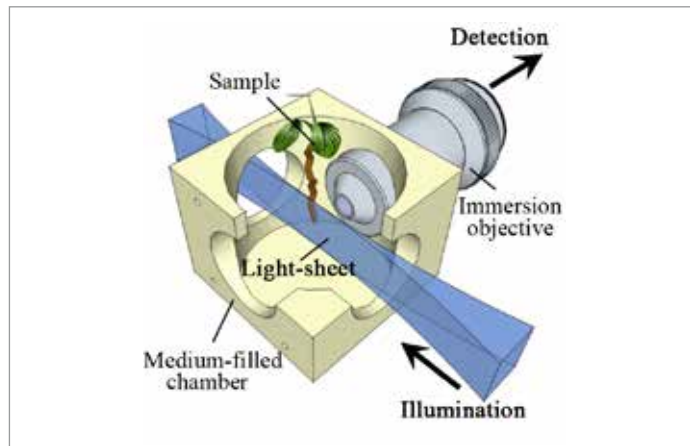


3. a) Sketch of the bar coating process. b) Atomic Force Microscopy map of the oriented film. c) Mobility plot versus gate voltages measured in the parallel and perpendicular direction with respect to the coating direction. d) Average saturation mobilities (circles) with their standard deviation (bars) for 56 FETs coated on an $8\times 8\text{cm}^2$ area in both parallel and perpendicular directions, compared to a distribution obtained from 8 spin-coated FETs.

IN VIVO CALCIUM IMAGING BY LIGHT SHEET FLUORESCENCE MICROSCOPY

Alessia Candeo - Supervisor: Cosimo D'Andrea

In the last decade, the study of the dynamics of intracellular calcium concentration $[Ca^{2+}]$ has been a main focus in life science. The role of calcium in cell physiology is crucial and its study requires the ability to monitor the dynamics of its concentration in living cells, with both spatial and temporal accuracy. In fact, the changes in the cytoplasmic and organellar calcium concentrations, that are induced by cell stimulation, occur with a defined pattern, which is fundamental for the functional outcome. As a result of this biological complexity, it is therefore not surprising that our understanding of calcium signalling has been largely dependent on the development of methodologies that can be used to monitor the calcium concentration in living cells. The advances of optical methods increased the attention on fluorescent indicators and microscopy development. Here I discuss the implementation of a novel microscopy approach aimed to monitor the calcium dynamics, named Light Sheet Fluorescence Microscopy (LSFM), and its applicability to two main issues: calcium dynamics in *Arabidopsis thaliana* roots and in Zebrafish brain. LSFM is a fluorescence microscopy technique where the illumination axis is perpendicular to the



1. Schematic of a LSFM setup: a single light-sheet is created on the sample, orthogonally to the detection axis.

detection axis (Figure 1). A laser beam is used to create a thin sheet of light in the focal plane of the detection objective. The acquisition is done through a fast camera, so that images are recorded in one shot and over a wide field of view. Still, since the lateral resolution of the system is given by the objective in use, it is possible to achieve cellular and subcellular details. By moving the light-sheet throughout the sample (or, vice versa, the sample through the light-sheet), 3D stacks of images can be acquired. Since the light-sheet can be a few micrometers thin, the out of focus fluorophores are not even excited, providing not only optical sectioning, but also a reduction

of the light dose received by the specimen. This results in a low phototoxicity of LSFM, which is the method of choice to make long term time-lapse imaging, without damaging the sample. In plants, calcium is involved in many aspects of development and takes part into different regulatory processes. Transgenic *Arabidopsis* plants expressing the genetically encoded-FRET-based calcium probe Cameleon were mounted vertically in quasi-physiological conditions in a chamber filled with hydroponic medium in the LSFM setup. In this case, the light-sheet was created through a cylindrical lens, while the detection path was equipped with a dual-wavelength system in

front of the CMOS camera for the parallel acquisition of the two FRET channels. To better understand the physiological role of specific proteins in the calcium signalling, I have monitored the intracellular responses, such as stimulus-induced calcium mobilization, on a large field of view, at single cell resolution and in physiological conditions for the root. The application of different stimuli gave rise to specific fingerprints in the signals.

In order to understand the physiological role of proteins building up calcium channels, I compared the signal from wild type plants with that of samples with knocked out proteins. Interestingly, knocked-out mutants showed deregulated calcium responses depending on the silenced protein. Moreover, for those mutants showing a clear phenotype in root hairs, that are fundamental indicators of the plant health and resistance, I examined the spontaneous calcium oscillations at the root hair apex during growth. The variations of calcium concentration proved to be correlated with the pulsatile elongation velocity of the hairs, with a time lag of few seconds. It can be hypothesized that the calcium increase is a regulatory mechanism that limits the turgor-driven expansion of the hair after each burst of elongation, preparing it for the following burst. A system where this feedback fails, leads to unhealthy plants. Calcium imaging is also becoming more and more significant for brain activity decoding. It is known that a complex interaction between spontaneous activity and

sensory-induced neural responses exists in the brain. In early studies involving evoked activity there was the wrong assumption that spontaneous activity is a random noise, averaging out during statistical analysis. On the other hand, recently it has been proved that spontaneous activity affects brain processing and behavior, since it partially accounts for the across-trial variability observed in neural responses and since it is spatiotemporally structured I then exploited LSFM to simultaneously detect neuronal firing across the brain of a zebrafish larvae expressing the genetically encoded calcium indicator GCaMP5. Zebrafish has become one of the most important models for functional neuroimaging, mainly thanks to its transparency at the larval stage, together with its small dimensions and its conspicuous number of neuron (~80000). For this purpose, a light-sheet was created by scanning a Gaussian beam by means of galvanometric mirrors. This allowed fast recordings of a wide field of view, with single cell resolution, from functionally different brain regions, with a phototoxicity more than 3 times lower than that of standard techniques, like confocal or 2-photon microscopy. I also implemented a two-photon LSFM for sensory-induced neural responses: in fact, exciting the fluorophores with infrared laser avoids unwanted visual stimulation and adaptation to visible light. I focused my attention on the acquisition of spontaneous calcium variations in the optic tectum, a model area for the study

of vertebrate visual circuits, at high framerate (100 fps). Though, this led to huge datasets (~500 GB for a 3 hours recording) that had to be analyzed through a High Throughput Computing system. The investigation showed that the spontaneous activity is organized in topographically compact assemblies of functionally similar neurons, reflecting the tectal retinotopic map, despite being independent of retinal drive. From a spatiotemporal point of view, we observed the presence of wave-like patterns. To conclude, light sheet fluorescence microscopy is well suited for the study of calcium dynamics in different samples and for different purposes. The possibility to look at the calcium concentration variations over a wide field of view with single-cell resolution and with sectioning capability makes LSFM a novel tool for in vivo calcium studies. Moreover, the far lower phototoxicity for the sample compared to standard microscopy techniques makes LSFM ideal for time-lapse experiments. The research leading to this PhD dissertation has been accomplished in the Physics Department of Politecnico di Milano, in collaboration with Università statale degli studi di Milano and IBENS (Institut de Biologie de l'École Normale Supérieure de Paris).

MOLECULAR AND NANOSCOPIC ORGANIC FILMS FOR PHOTODETECTION

Lorenzo Caranzi - Supervisor: Prof. Guglielmo Lanzani

The interest on molecular and polymeric semiconductors as materials for electronics has grown rapidly in the last decades. Organic semiconducting materials offer the possibility to be processed with solution-based techniques at low temperatures, allowing their deposition on flexible and low cost plastic substrates. These features, together with the good absorption in the visible range, make possible to realize unconventional light sensing devices with excellent performances. Moreover, high optical cross section and the ease to deposit thin films from solution open up the possibility to obtain organic transparent photodetectors for window-integrated electronics and smart displays. My Ph.D. dissertation reports on the development and characterization of organic photodetectors based on nearly transparent, nano-dimensioned active layers.

Firstly, the possibility to obtain a photoactive molecular junction based on self-assembled monolayers (SAMs) of indoline dyes sandwiched between two electrodes was demonstrated. The bottom aluminum contact presents a native oxide where the carboxylic acid group of the molecule can bind, while the top contact is a transparent conductive polymer (PEDOT:PSS).

The formation of the SAM was investigated: RAIRS measurements show that the molecule form a chemical bond with the bottom aluminum electrode, while UV-Vis absorption measurements provide a quantitative evidence of the presence of a SAM. Despite the very low optical density of the SAM (less than 1% of photons absorbed), the molecular junction generates a photocurrent when exposed to visible light. The EQE spectra shows that the photogeneration mechanism involves unambiguously the molecular monolayer, since the photoresponse can be tuned using dyes with different absorption spectra (D102, D133 and D205). As shown by electro-optical characterization, this device is characterized by a large dark/ photocurrent ratio in short circuit conditions, an important aspect for highly photosensitive molecular photodetectors. In particular, a maximum V_{oc} of 180 mV with dye D205 and a maximum J_{sc} of 47 nA cm^{-2} with dye D102 were obtained. The dynamic response of the junction is limited by the nature of the contacts as well and can be improved by enhancing the conductivity of the top electrode. With the addition of a semi-transparent gold layer on top of the polymer a minimum time constant of $35 \mu\text{s}$

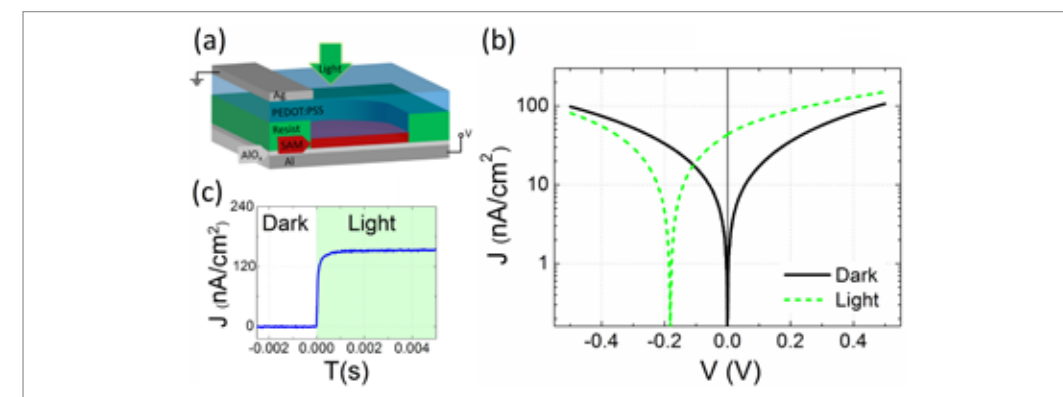
is obtained for the rising edge of the photoresponse. Considering the realization of nano-structured photodetectors, the molecular junction presented here not only allows for the implementation of semi-transparent photosensitive devices, but it represent also an instrument to investigate charge photoexcitation, separation and collection at the interface between molecular monolayers and electrodes, still requiring a deeper comprehension.

In the second part of the work, a planar photodetector based on a transparent donor/acceptor organic couple was developed and characterized. This device is based on a bottom layer of the n-type polymer P(NDI2OD-T2) which acts as electron transport layer, and a top layer of a p-type squaraine based dye. Despite the very low optical density (< 5% of photons absorbed) shown by the active bilayer, the External Quantum Efficiency of this device exceeds 100% when biased at 100 V, showing a photoconductive gain of 25.9. The presence of the squaraine dye introduces energy trap states for the positive charges, allowing for the circulation of electrons through the n-type polymer. The fabrication of a phototransistor was carried out with the addition of a polymeric dielectric and a

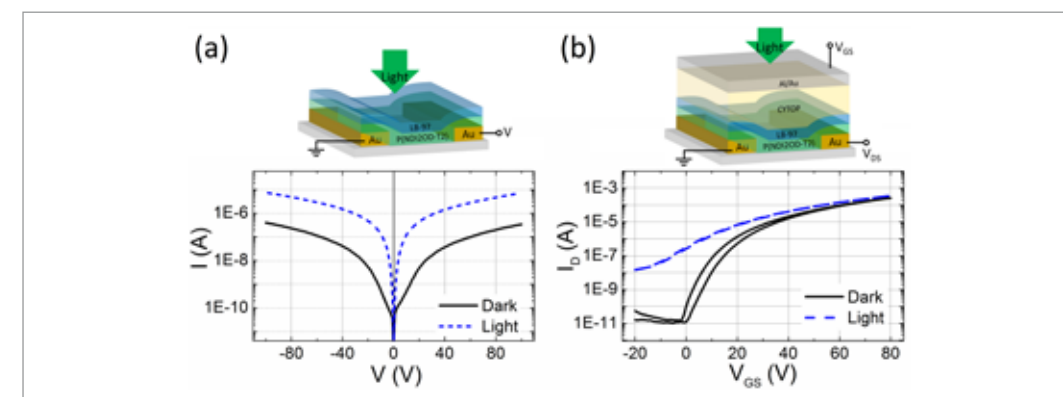
semi-transparent gate electrode on the planar photodetector configuration. The transistor shows n-type behavior and electron mobility in saturation regime of $0.12 \text{ cm}^2 \text{ V}^{-1} \text{ s}^{-1}$, consistently with devices made with the pristine P(NDI2OD-T2). We characterized the opto-electronic properties of the transistor in terms of photoresponsivity and dynamic response. The phototransistor shows a responsivity of 48 A W^{-1} , two orders of magnitude higher than the responsivity of the planar

photodetector structure. This is due to the electrical gating effect, which fosters both the electron mobility and the injecting capability in the active layer. Photocurrent maps were obtained for both devices, giving fundamental information on the evolution in time of the photoresponse coming from a specific area of the device. Depending on where photocurrent is localized, the photocurrent contributions at different frequencies can be assigned to different

photogeneration mechanism, such as photoinduced electron injection, photoconduction or photovoltaic regime. Together with the development of a broadband, high responsivity photodetector based on a nearly transparent active material, this work provides a further contribute to a better comprehension of the mechanisms underlying photogeneration in these device architectures.



1. Structure of the photoactive molecular junction (a). JV curves of the molecular junction made with D205 in dark conditions and under illumination (LED at 505 nm) (b). Transient of the photocurrent in time ($V = 0 \text{ V}$) (c).



2. Structure of the planar photodetector based on the nearly transparent bilayer, with the related IV curve in dark conditions and when exposed to polychromatic light (a). Structure of the phototransistor and related trans-characteristic in dark and under polychromatic light condition ($V_{ds} = 80 \text{ V}$) (b).

HIGH-PRECISION MOLECULAR SPECTROSCOPY WITH OPTICAL FREQUENCY COMBS

Marco Cassinero - Supervisor: Nicola Coluccelli

Optical frequency combs (OFCs) revolutionized the field of frequency metrology by enabling the first direct and phase coherent link between the domain of the radio frequencies (RF) and that of the optical frequencies (THz). An OFC can be seen as an array of thousands phase-coherent single-frequency lasers emitting at discrete and evenly spaced frequencies (comb teeth). The optical frequency ν_n of each comb tooth is defined by three parameters, namely the tooth order n (an integer of order 10^5 - 10^6), the comb frequency spacing f_r , and the offset frequency f_{CEO} , through the simple relation $\nu_n = n f_r + f_{\text{CEO}}$. Both the teeth spacing and offset frequency range in the RF from tens of MHz up to tens of GHz according to the OFC system configuration. When both of these quantities are linked to a primary frequency standard, like the notorious Cesium clock operating in the RF domain, the comb is said to be fully referenced and it becomes an optical ruler. This optical measuring tape has opened the road for a wide range of new applications where accuracy, precision and speed are fundamental aspects. The work of this thesis is aimed at the development of innovative techniques and instrumentations for high-resolution molecular spectroscopy in the near (NIR) and mid (MIR) infrared spectral regions

employing OFCs.

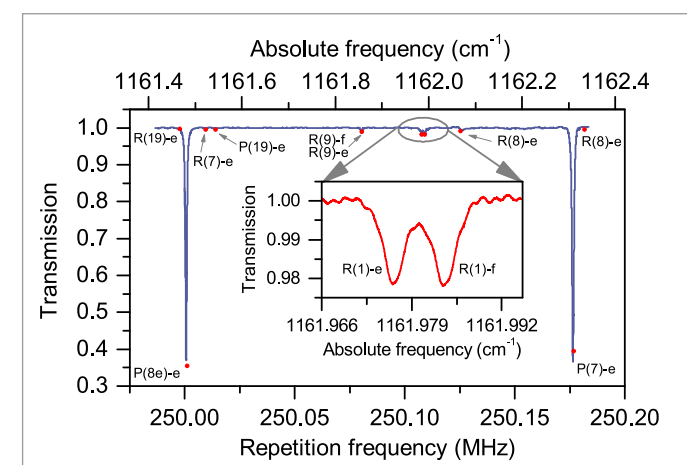
In these spectral regions, from 1.5 μm to 12 μm , molecules show the strongest absorption features and precision spectroscopic measurements lead to a deep understanding of the molecular physics such as the determination of the fundamental constants and their variations over time. The first challenge addressed in this Ph.D. work was to extend a commercial optical frequency comb synthesizer based on a dual branch erbium fiber femtosecond source emitting at 1550 nm to cover the aforementioned spectral regions. The synthesis of the MIR comb was based on a Difference Frequency Generation (DFG) process. The main output of the Er: fiber oscillator at 1.55 μm (50 fs long pulses with an average output power of 550 mW) is used as the pump radiation for the DFG process in a 1-mm thick GaSe non-linear crystal, whereas the second output, a tunable self-frequency-shifted soliton in the 1.76–1.93 μm range (90 fs pulses with an average power varying from 100 to 250 mW depending on the wavelength), is used as a signal for DFG. The generated MIR OFC covered an extremely large 8–14 μm wavelength range with average output power of few mW. Spectroscopy techniques employing frequency combs can be divided

into two major categories: comb assisted narrow band and direct comb broad band. In the former configuration the frequency comb is used as a measuring tape. A single wavelength laser (CW) is referenced to the frequency comb by making it interfere with a comb tooth. The resulting heterodyned beat-note is compared to a RF reference and the error signal is used to lock the CW laser to the N-th comb tooth. The absolute frequency is then always known. The f_n of the comb is then swept in frequency and for each step the CW frequency follows the N-tooth. The final result is the same as sweeping the CW laser wavelength. The CW laser is sent through a gas filled cell and the transmitted light is recorded for each f_r frequency step. I used this technique to lock a quantum cascade laser (QCL) emitting at 8.6 μm to the frequency comb generated by the DFG process. Fig. 1 shows the results of a 30 GHz CW laser scan performed on a gas cell filled with N_2O . An impressive 1400 SNR has been achieved so as to clearly resolve lines with a relative absorption intensity of just 2%. The ultimate relative accuracy of the line center frequencies is 3×10^{-10} limited only by the pressure sensor and can be lowered down to the limit of the locking system to the 2×10^{-12} level

with a better sensor.

In the latter spectroscopy technique, the frequency comb is employed as the probe source directly and a way to distinguish the amplitude of the various teeth is necessary. In this sense a lot of approaches has been developed. Notable examples are FTIR, grating separation (VIPA) and Fabry P erot vernier cavities.

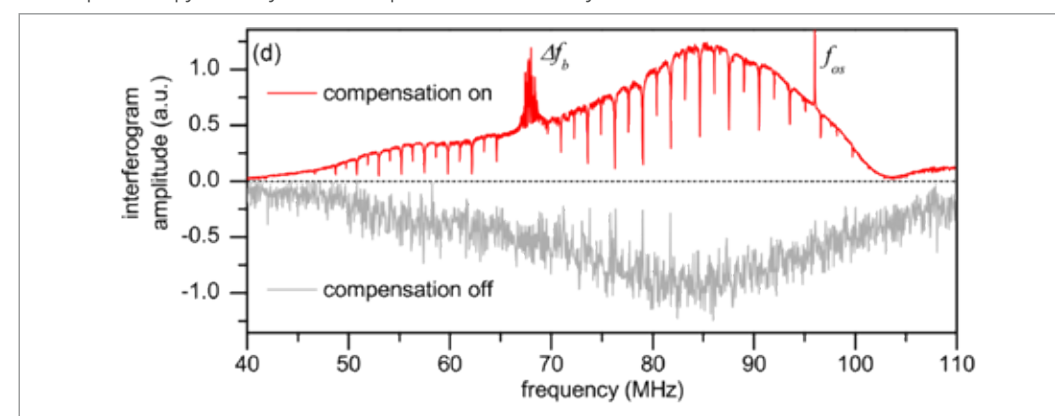
An innovative and interesting technique called dual comb has been recently explored. It employs two combs: the first one with a certain f_{r1} is sent through the gas while the other has a slightly different repetition rate $f_{r2} = f_{r1} + \Delta f_r$ and is combined with the first one, after the cell, onto a photodetector. The Fourier transform of the acquired signal shows a frequency comb structure in the RF domain with tooth spacing of Δf_r , i.e. the beat-note between each tooth of the first comb with the respective tooth of the second comb. The final result is then that the first comb has been heterodyned to the RF domain and the intensities of the various teeth are already separated. The usual way to perform a dual comb spectroscopy is to fully



1. N_2O transmission spectrum. Absolute frequency (top scale), comb rep rate (bottom scale). Red dots: HITRAN calculated absorption-peaks. Inset: detail of a doublet with a 2% peak fractional absorption.

stabilize, i.e. both the f_r and f_{CEO} of the two combs to RF or optical references but requires a lot of efforts and is doable only in a lab environment. I developed an approach where both combs are in free running, completely unlocked. The frequency jitter is acquired in a separate way and the spectroscopy signal is corrected in an analog fashion, with mixers, with the signal carrying the jitter. The importance of this compensation and the performances of the system has

been tested with a measure on a C_2H_2 cell and are shown in fig. 2. The absorption lines with the compensation off are completely washed out while with the compensation on they are clearly visible. The final accuracy was measured to be ± 98 MHz with a detection limit of 60 ppm. The sensitivity can be greatly improved by increasing the interaction length of the probing laser with the gas, for example in a multi-pass cell.



2. Jitter-compensated spectrum obtained by FFT of the averaged acquired signal (top red curve), compared to the free running single-shot spectrum (gray curve, inverted for clarity).

COLLECTIVE EXCITATIONS IN HIGH TEMPERATURE SUPERCONDUCTING CUPRATES STUDIED BY RESONANT INELASTIC SOFT X-RAY SCATTERING

Greta Dellea - Supervisor: Prof. Giacomo Ghiringhelli

Since the discovery of high temperature superconductors (HTS), more than a quarter of century ago, increasing efforts have been devoted to the search of the basic mechanism leading to superconductivity, but a conclusive and generally agreed explanation is still missing. In this scenario, a better understanding of collective excitations in layered cuprates, either competing or coexisting with the superconducting state, has become a fundamental issue. Cuprates are characterized by the presence of CuO_2 planes – Cu^{2+} ions alternated to O^{2-} ions – separated each other by blocking layers; much of the physics of cuprates takes place in these planes. The parent compounds have one hole per Cu site and the strong electron correlation, typical of transition-element oxides, leads to insulating behavior. These localized holes order antiferromagnetically (AF) and the resulting spin dynamics is well described in terms of spin wave, or magnon, excitations within the bidimensional spin $\frac{1}{2}$ Heisenberg model. When the insulating parent compounds are doped, the additional dopant charges rapidly destroy the Néel ordering and trigger the superconducting transition in correspondence to a critical doping range. If the doping is further increased, the system

reaches a non-superconducting metallic phase where low energy electronic excitations have Landau Fermi liquid-like properties. A boost in the interest in collective spin excitation and their evolution with doping came from recent experimental results and theoretical calculations, suggesting a pairing by exchange of magnetic excitations, in concomitance with the development of resonant inelastic x-ray scattering (RIXS) at Cu-L_3 edge, which has been proved to be the optimal technique to study magnetic, orbital and charge fluctuations in the CuO_2 planes. RIXS in the soft x-ray regime is an energy loss spectroscopy, in which the incoming photons energy is tuned at an absorption edge. The signal enhancement at the resonance can be very large, making the measured inelastic signal strong enough to be detected. The choice of the absorption edge also provides chemical selectivity and stringent selection rules on the type of excited states created in the scattering process, mainly if the polarization of the photons is known and controlled. Finally, the sizable momentum carried by x-ray photons can be taken into account to measure the energy vs momentum dispersion relation of the excited states. This thesis presents some of

the results obtained with Cu-L_3 RIXS on superconducting and insulating cuprates during my activity in the group of Prof. G. Ghiringhelli and Prof. L. Braicovich of the Physics Department of Politecnico di Milano (Italy). The group has a well-established experience in synchrotron-based spectroscopies for the study of magnetic and electronic properties of transition-elements and rare-earth compounds. Recently they focused their activity on RIXS, contributing to the development of the technique, both from the point of view of science and instrumentation. Starting from the experimental evidence that optimally doped high- T_c superconductors exhibit high-energy damped spin excitations (paramagnons) with dispersions and spectral weights closely similar to those of magnons in undoped cuprates, we extended our analysis to a large family of cuprates; spin excitations have been detected in a wide class of samples and dopings, from the well know bulk crystals and thin films, to more complex superconductors, obtained by superlattices and heterostructures, down to a few unit cells layers and nanopatterned structures, giving a further confirmation of the robustness of magnetic excitations and

providing an ubiquitous ingredient for the superconductivity. We also used RIXS to measure the evolution of (para)magnons across the entire phase diagram of hole-doped cuprates, from the superconducting underdoped and optimally doped, to the non-superconducting highly overdoped samples. These results suggest a more complex explanation of the pairing mechanism, that could include the influence of the low-energy magnetic excitations, and other ordering phenomena. Superconductivity could be achieved by doping with both holes and electrons. The e-doped region of the cuprates phase diagram has been less investigated so far, mainly due to technical limitations in sample growth and experimental techniques. Changing the sign of the doping carriers has strong implications for the shape of the corresponding phase diagram and some important physical proprieties, such as pseudogap, stripe order and maximum critical temperature (T_c), dramatically change. In that sense, the asymmetry between electron- and hole-doping in high- T_c cuprates is fundamental in understanding the processes at the basis of the superconducting transition. In this thesis we show RIXS spectra measured from the archetype e-doped $\text{Nd}_{2-x}\text{Ce}_x\text{CuO}_4$ (NCCO) crystal and from the more exotic $\text{Sr}_{1-x}\text{La}_x\text{CuO}_2/\text{GdScO}_3$ infinite layer cuprate heterostructure. Our data show a magnetic excitation hardening under e-doping in stark contrast with h-doping; this result is counterintuitive and interpreted in terms of a strongly itinerant character compared to the more

localized spin dynamics found in h-doped cuprates.

It is also interesting to notice that both artificial h- and e-doped superconducting cuprates perfectly mimic the collective excitation behavior of the corresponding bulk crystals, envisaging the possibility to explore general properties of HTS physics on a broad range of conditions, by means of artificial compounds not constrained to the thermodynamic limitations governing chemical stability of bulk materials. Our results suggest that any successful theory for HTS should require a detailed understanding not only of the magnetic excitation spectrum, but also of the combined effect of electron-phonon coupling and charge-order in the normal state from which superconductivity emerges. We found increasing general evidence that, in cuprates, spin excitations get coupled to both lattice modes and charge order. A better clarification of this three-actor scenario for the superconductivity pairing mechanisms will require further systematic use of high resolution resonant elastic and inelastic x-ray scattering. So far all the results discussed have been acquired with two high resolution RIXS spectrometer, both designed and build by our group: AXES (Advanced X-ray Emission Spectrometer) working since 1995 at the beamline ID08 of the European Synchrotron Radiation Facility (ESRF) and now dismissed, and SAXES (Super-AXES) which is the evolution of AXES, and has been installed in 2006 at the ADRESS beamline of the Swiss

Light Source (SLS). At present, the scientific output of soft-RIXS is reaching its limits due to technical limitations in terms of energy resolution, signal intensity, outgoing polarization analysis and sample orientation control. In order to overcome all these limitations, the new ERIXS (European RIXS) instrument at the new ID32 beamline of the ESRF has been designed and commissioned and it is now ready for the first user experiments run. The final part of my PhD work has been mainly devoted to the commissioning and performances characterization of the new spectrometer, which now holds the world record of resolving power with a total instrumental resolution of 55 meV at Cu-L_3 edge (930 eV). This thesis reports a detailed instrumentation session, with preliminary experiments on antiferromagnetic and superconducting layered cuprates, and test measurements at different edges: Ni-L_3 , Mn-L_3 , Ti-L_3 , Ce-M_3 , Gd-M_3 , Eu-M_3 , extending the class of materials that can be investigated by RIXS, from the more studied cuprates, to a wide range of systems.

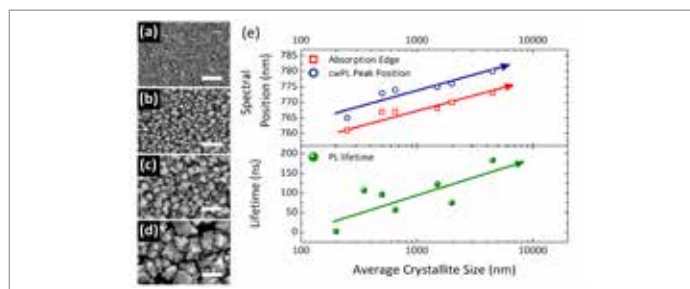
PHOTOPHYSICS OF HYBRID LEAD-HALIDE PEROVSKITE: ABSORPTION AND LUMINESCENCE PERSPECTIVES

Valerio D’Innocenzo - Tutor: Prof. Guglielmo Lanzani
Supervisor: Dr. Annamaria Petrozza

After being successfully employed in photovoltaic devices, hybrid organic-lead halide perovskites are now emerging as promising materials for light emitting devices. The understanding of the optical properties of these materials is an urgent issue to be addressed in order to boost the development of perovskite based laser devices. Recently it was demonstrated that the photoluminescence (PL) dynamics in $\text{CH}_3\text{NH}_3\text{PbI}_3$ (MAPbI₃) thin films are driven by a radiative non geminate (bi-molecular) electron-hole recombination process, also involving a monomolecular trap induced non radiative decay path. For this reason the excited carrier population temporal evolution $n(t)$ can be modeled by taking into account a bi-molecular intrinsic radiative recombination coefficient (B_{rad}) and a non-radiative monomolecular trapping rate (A), i.e. . Another interesting observation is the incredibly long PL lifetime found for the Cl doped MAPbI₃, reaching up to hundreds of ns, previously associated to micrometer long photo-carriers diffusion length. While initially such a long lifetime was associated to the presence of Cl ions within the perovskite unit cell, subsequent studies showed that Cl is mainly expelled from the

perovskite films. Nevertheless its presence drives the crystallization inducing the formation of larger crystals with anisotropic shape. These observations highlights an important unexplored issue of the relationship between structural and light emission properties in these self-assembled compounds. The aim of the work presented is to fill this gap reporting an investigation of the influence of MAPbI₃ thin film morphology on

all the samples. Interestingly this data clearly show that as the polycrystallite grows in size, the optical absorption edge shifts to lower energies (longer wavelength) along with the PL peak position, thus keeping the Stokes shift constant. We then performed time resolved PL measurements (tr-PL) in order to obtain the PL lifetimes as a function of the average crystal size (bottom panel of figure 1.(e)). As the average crystallite size



1. (a)-(d) Top View SEM images of MAPbI₃ grown in different conditions; scale bars: 2 μm. (e) Spectral position of the UV-Vis absorption band edge, peak position of cw-PL (top) and PL lifetime (bottom) as function of the crystallite size.

the luminescence properties. In Figures 1.(a)-(d) the top-view SEM images of four samples with an observed average size of the crystallite dimension ranging from < 250 nm to > 2 μm are reported. In the top panel of figure 1.(e) we report the position of the optical band edge obtained from UV-Vis absorption spectra together with the position of the peak of PL of

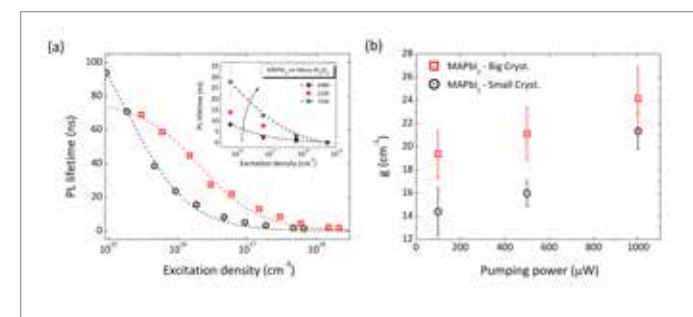
increases we observed nearly two order of magnitude increase in the lifetime going from 2 ns for the smallest crystallites (< 250 nm) to more than 100 ns for the largest ones (> 1 μm). The excitation density dependence of PL lifetime for two representative sample (with crystallite dimension < 250 nm and > 1 μm respectively) is reported

in figure 2.(a). According to the relaxation model proposed, the PL lifetime dependence on the initial excitation density (n_0) can be written as:

$$\tau_{\text{PL}} = 1/(A + B_{\text{rad}} \cdot n_0) \quad (1).$$

By fitting Equation (1) to the experimental data we estimate the intrinsic bi-molecular radiative recombination rate for both the samples. We find that larger crystallites exhibit lower radiative recombination coefficient, $B_{\text{rad}} = (0.62 \pm 0.06) \cdot 10^{-9} \text{ s}^{-1} \text{ cm}^3$, with respect to the smaller ones, $B_{\text{rad}} = (3.7 \pm 0.2) \cdot 10^{-9} \text{ s}^{-1} \text{ cm}^3$ while the monomolecular trapping rate A is only slightly affected, $1.3 \cdot 10^7 \text{ s}^{-1}$ to $0.72 \cdot 10^7 \text{ s}^{-1}$ as the crystallite dimension decreases.

Thus the red shift of the band edge observed with increasing crystallite size (figure 1.(e)) is accompanied by the reduction in the radiative recombination coefficient B_{rad} revealing a correlation between the semiconductor band-gap E_g and the intrinsic radiative bimolecular recombination rate B_{rad} . Intriguingly intensity dependent PL measurements, while lowering the sample temperature shows the same trend (inset in figure 2.(a)), thus suggesting that the temperature reduction and increased crystallite size are inducing the same changes in the electronic structure. Both these observations can be explained in term of the Pb-I cage relaxation. In fact it has already been shown that a reduce strain of the I-Pb-I bonding angle in this material can induce both a red shift of



2. (a) PL lifetime as a function of the excitation density for small (black dots) and big (red squares) crystallites MAPbI₃ sample. Dashed lines represent the curves obtained fitting the relation (1) to the data. In the inset the PL lifetime as a function of initial excitation density for Meso-MAPbI₃ at 220 K (red circles) and 150 K (green squares) respectively. (b) Optical gain for the same samples. The error bars refer to the 95% confidence intervals of the fitted parameters value.

the band gap and a reduction of the bimolecular radiative recombination coefficient. These findings are of extreme interest considering the potential employment of these materials for lasing applications, since a longer lifetime would create larger steady state population under cw illumination, beneficial for low threshold CW lasing. Another important parameter that determines the lasing threshold is the optical gain coefficient of the material. For this reason we performed optical gain measurements on the two samples mentioned above using the established variable stripe length method. In this experiment the PL intensity $I(\lambda, l)$ collected exciting the sample with a striped shape excitation is related to the stripe length l by the following:

$$I(\lambda, l) = \frac{A(\lambda)I_p}{g(\lambda)} (e^{g(\lambda)l} - 1)$$

where A is a constant related to the spontaneous emission cross

section, I_p is the intensity of the pump, g is the gain coefficient, and λ is the emission wavelength. The optical gain values as a function of the incident pump intensity, reported in figure 2.(b), were extrapolated fitting the PL measurements to equation 2. We notice that the gain is consistently higher in the case of larger crystals at any of the considered pump power. In conclusion, with this work we demonstrated that by controlling the crystallization procedure it is possible to engineer the semiconductor band-gap and the intrinsic radiative lifetime together with the optical gain of the compound. Eventually the longer PL lifetime and higher optical gain, characterizing larger crystals MAPbI₃ allow us to suggest that this crystalline morphology must be preferred for the realization of lasing devices.

GRAPHENE AND PHOSPHORENE BASED FIELD EFFECT TRANSISTORS

Marco Fiocco - Supervisor: Roman Sordan

The continuous evolution of silicon-based electronic devices has granted 40+ years of development in telecommunications and digital electronics. The performance improvement, correctly predicted by Moore's law, is currently slowing down: the increased importance of short channel effects and the physical limits in the scaling of MOSFETs are pushing the scientific community towards new research fields, looking for a new material that can replace silicon. Within this framework, the discovery of graphene and its very interesting physical properties gathered a lot of attention.

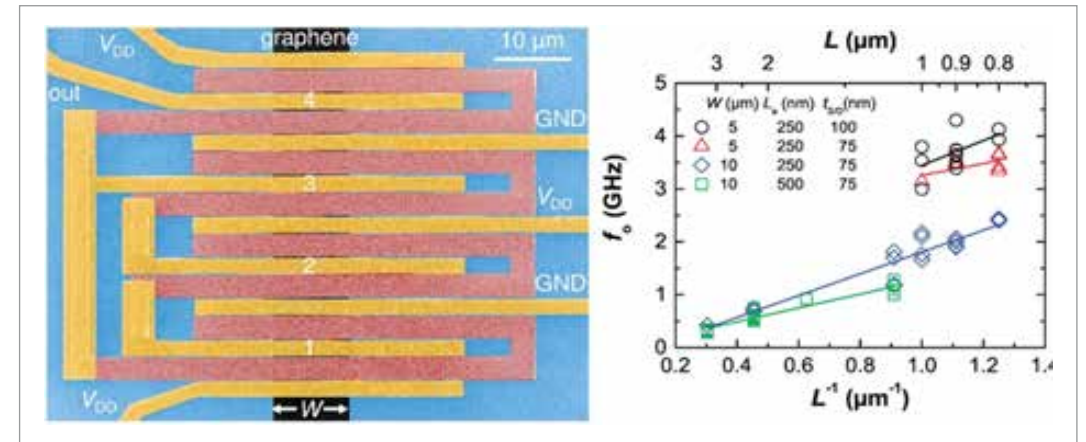
Monolayer graphene is a stable two-dimensional (2D) layer of carbon atoms arranged in a hexagonal lattice and can be seen as a single basal plane of graphite. The hexagonal cell of graphene implies a peculiar band structure in which valence and conduction band touch in the area where conical-shaped bands are formed. For this reason, graphene is addressed as a semimetal or a zero-gap semiconductor; conically-shaped bands imply a linear dependence of energy on momentum, therefore describing charge carriers in a relativistic framework as massless Dirac fermions.

High grade crystallinity and absence of back-scattering

in graphene monolayers are the two main reasons for the high mobility values reported in literature for both gated and suspended devices. This fundamental property, combined with ambipolar conduction, field effect and graphene's intrinsic 2D nature have pushed the scientific community towards the realization of simple and complex graphene-based circuits. However, the absence of a band-gap restricts graphene's potential applications to high frequency electronic devices, since a proper off-state is required for logic applications. The pioneering work on graphene has been a cornerstone for a new field of solid state physics focused on the study of other novel 2D materials. Such materials are also currently being studied for logic applications, trying to overcome limitations of graphene. The materials holding most promise are transition metal di-chalcogenides (TMDCs) and phosphorene: while TMDCs show low mobility values, most of the attention is currently on the latter, a high pressure allotrope of phosphorus showing high hole mobility values and thickness-dependent band-gap. This thesis focuses on realization and characterization of graphene and phosphorene based electronic devices. Using graphene grown

by chemical vapor deposition, electron beam lithography and metal contact evaporation, a wide range of graphene-based field effect transistors (FETs) have been realized: starting from simple FETs, inverters have been realized showing voltage gain up to 12. Using graphene-based inverters as building blocks, more complex ring oscillators (ROs) have been realized.

ROs are test-bed for investigating materials for possible application in electronics since they can provide information on the high frequency performances of such new materials. The realized devices were made of 3 inverters cascaded in a loop: if each inverter stage shows a gain greater than 2 and is capable of driving the following inverter, the system oscillates at a native frequency that depends on the material properties and fabrication parameters. An extensive study on scaling of ROs was carried on, addressing the role of channel width, source/drain thickness and gate length. By systematic reduction of gate length, it was possible to increase the oscillation frequency from the MHz range to a record value of 4.3GHz for 800nm gate length. Further scaling with gate length below 700nm yielded no working devices: in this range non-scalable resistances (like contact resistance)



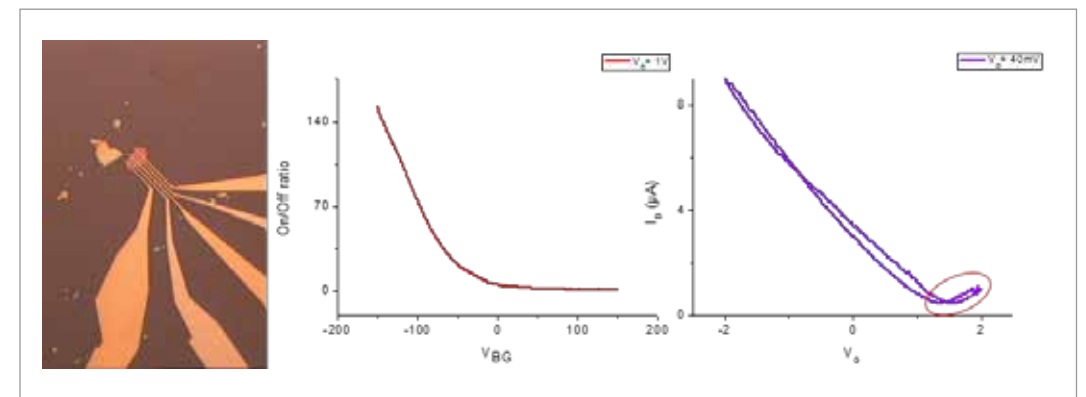
1. On the left, a ring oscillator built with 3+1 cascaded inverters. On the right, scaling rules of oscillation frequency

become dominant, limiting gain of inverters and preventing ROs from oscillation.

Regarding phosphorene, flake fabrication through exfoliation from black phosphorus crystals with scotch tape technique was optimized. An extensive characterization of flakes' thickness and ambient stability was carried on by means of atomic force microscopy, underlining the difficulties of obtaining flakes thinner than 10 nm. The rapid

ambient degradation of air-exposed flakes represents a critical problem to be addressed for device fabrication. Using exfoliated black phosphorus crystals, electron beam lithography and metal contact evaporation, a wide range of back-gated and top-gated devices were realized and characterized. The simple fabricated FETs exhibited on/off ratios up to 150, with mostly hole conduction. Occasional ambipolar behavior holds holding promise

for the realization of phosphorene-based inverters. Degradation of ambient-air exposed flakes limits potential electronic application and requires therefore a feasible flake passivation. Within this work of thesis, overlapped structures (completely covering active material) and PMMA coverage served as partial passivation, granting an extended period of measurability for the samples.



2. On the left, an image of a typical top-gated phosphorene device; on the right, the best on/off ratio obtained and a plot showing ambipolar behavior in one of the samples.

LIGHT HARVESTING AND MANIPULATING COMPONENTS FABRICATED BY FEMTOSECOND LASER MICROFABRICATION IN OPTO-FLUIDIC LAB ON CHIP DEVICES

Sameer Guduru - Tutor: Prof. Guglielmo Lanzani

Supervisor: Dr. Francesco Scotognella, Dr. Krishna C Vishnubhatla

Motivation

Lab on chip (LOC) devices have revolutionized sensing capabilities and hence have found varied applications ranging from bio-hazard detection to synthesis of drugs, creating integrated sources of light, fluorescence detection etc. This is due to the fact that, the field of microfluidics plays a central role in LOC devices, which basically deals with the transportation and manipulations of very small quantities of liquid analytes in micro-capillary structures in a substrate with dimensions of a few millimetres. The main advantages of the microfluidic devices are as follows

- 1) Reduced consumption of reagents
- 2) High sensitivity
- 3) Ease of transportation of liquids from one end of the chip to the other
- 4) Re-configurability of the devices, whose properties can be altered changing the analyte

Such interesting properties can be exploited in realizing components in the direction of micro total analysis applications (u-TAS). Such u-TAS systems require a high level of integration in order to achieve many functionalities such as optical, electrical etc. in the same device. However, using the traditional techniques used in

micro electro mechanical systems (MEMS) fabrication, realizing devices with such high level of integration, is cumbersome and not easy, as they involve multiple steps. Techniques like photolithography involve customization and optimization of masks and templates, in addition to the actual steps of fabrication. This renders the techniques not so useful in fast prototyping and small scale production. Hence, there is a need to explore new ways of fabrication with a fast turnaround time and the ease of making prototype.

Introduction to femtosecond laser micro-fabrication (FLM)

Hirao et al for the first time in 1996 demonstrated the use of tightly focused ultrafast lasers in creating microstructures through refractive index modifications in transparent dielectric structures like fused silica. In essence a focused femtosecond laser can be used like a pen and one could irradiate 3D patterns inside the bulk of transparent materials by translating the substrate below. This modification of the refractive index is restricted to the focal volume, thanks to the very high intensities of the order of Terawatts in the focal volume. Such high intensities leads to

optical breakdown through non-linear optical mechanisms like multi-photon absorption, tunnelling ionization and avalanche ionization. This non-linear nature of the processes can be exploited and any material, opaque or transparent can be micro-machined. The nature of material modification changes with laser fluence, leading to smooth refractive modification for lower values, enabling the fabrication of buried waveguides, and a birefringent refractive index modification for higher values, which assists in wet chemical etching to realize embedded micro-channels and similar structures. Moreover, due to the inherent 3D capability of the technique, the alignment procedures of the microstructures in the chip are completely eliminated along with other masking steps.

My activity

The activity during the course of PhD involved, the design, fabrication, and characterization of structures for light harvesting and manipulation in integrated, monolithic, opto-fluidic LOC architectures.

Light harvesting application Waveguide arrays in light harvesting

In the first application of light harvesting, an array of degenerate

waveguides and a microchannel were fabricated in close vicinity with each other using the (Femtosecond laser irradiation followed by chemical etching (FLICE) technique (also used in the other LOC configurations. The motivation of fabricating such a chip was to analyse and demonstrate the functioning of the FLM waveguide array, which is efficient in transporting fluorescent light from the excited dye in the microchannel in its vicinity, to the external end face of the chip. Such architectures can be utilized in the future in realizing on chip light sources and in transporting light from one part of a chip to the other for further analysis and manipulation.

Binary Fresnel lenses (BFLs) in light harvesting

Fluorescence detection and based sensing is widely used in many applications, however due to sub optimal quantities, it is hard to collect and investigate. Many devices have been demonstrated which act as fluorescence detectors, however, the level of integration is limited to only one or more of the component in the microfluidic chip like the filtering or both the excitation and filtering. In the quest of realizing a highly compact, monolithic and portable detector and in order to reduce the number of external components for detection, we designed, fabricated and validated such an integrated device. Such a device, contains the excitation element in the form of an optical fibre, a filter in the form of a 1D photonic crystal and finally a harvesting element in the form of a BFL. The microfluidic network and the BFL

are fabricated by FLICE and FLM respectively, while the 1DPC was fabricated using RF magnetron sputtering. The device was tested for its functioning and the limits of detection were established

Light manipulation applications Embedded semi-transparent microelectrodes

Microelectrodes have found varied applications in applications like di-electrophoresis, magento-hydrodynamics, on chip NMR etc. More so, introducing an additional feature of transparency to the electrodes, enables imaging through them and can be useful in real time analysis. 3D embedded electric structures using FLM have been demonstrated in the past, however, they are fabricated using either liquid metals or metallic alloys. Similarly transparent electrodes also have been demonstrated using FLM and a meh architecture, while in the former, the fabrication is restricted to the surface, the latter has a problem of non-uniform electric field strength distribution. In order to overcome these issues and in order to realize a truly embedded 3D transparent electrode, two widely used microfabrication techniques of FLICE and inkjet printing were synergized. While the FLICE was used to realize the microchannel architectures, the inkjet printing was used to fill in these micro-channels with transparent conductive polymeric inks to realize the electrodes and external connections. The functioning of the electrodes was demonstrated by filling a microchannel sandwiched

between both the electrodes and by applying a field across it. The microchannel containing liquid crystal molecules (LCMs) acts as a waveguide to the light coupled coaxially in the chip using an optical fibre. On the application of an electric field, the waveguide behaviour is lost, due to the change in the orientation of the LCMs and the light gets scattered away, demonstrating the functioning of the electrodes.

Simulations on the transmission properties of plasmonic heavily doped semiconductor based dielectric photonic structures

Embedded heavily doped semiconductor nanocrystals have tunable plasmonic behaviour in the near infra-red region of the EM spectrum, which is a function of the carrier density. Incorporating such nanocrystals in the matrix of 1D photonic crystals enables a way to modulate their transmission properties, by modulating their carrier density which in turn modulates their dielectric function. A selective tuning of the localized surface plasmon resonance in the NIR modifies the refractive index contrast in the photonic structure, consequently affecting the intensity and position of the photonic band in the visible spectral range. Such devices pave way for modulation of transmission post fabrication and enable realization of devices like electrochromic windows etc. Such devices can also be integrated into monolithic optofluidic devices enabling dynamic modulation of their transmission.

TWO-DIMENSIONAL ELECTRONIC SPECTROSCOPY IN THE ULTRAVIOLET

Aurelio Oriana - Supervisor: Prof. Giulio Nicola Cerullo

Two-dimensional electronic spectroscopy (2DES) is a powerful spectroscopic technique which allows to study the structure of the electronic states of a system and the dynamics of couplings or energy transfer between electronic states in time. 2DES can be seen as an extension of the standard pump-probe technique, with the extra capability of resolving the pump frequency dependence of the transient absorption signals. The principle of 2DES is the following: the system under analysis is excited by three consecutive pulses, two pump pulses and one probe pulse, with relative delays which are experimentally controllable. This pulse sequence creates a macroscopic third-order nonlinear polarization that emits a field, following the last pulse. By a double Fourier transform of the generated signal one derives the 2D spectra as a function of pump frequency and probe frequency. With respect to standard pump-probe, where excitation with a broadband pulse limits selectivity, 2DES preserves both temporal and spectral resolution. 2DES in the visible is used to study photosynthetic light harvesting complexes and molecular aggregates, and its extension to the UV range is extremely promising for the study of biomolecules such as DNA and proteins.

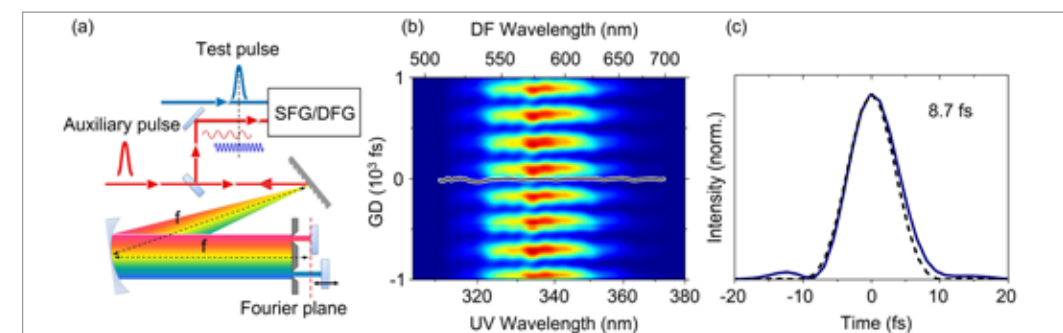
The aim of this thesis is to present the development of a 2DES setup in the UV range. Two main challenges need to be overcome in order to realize such an experimental setup: first of all, the generation of ultrabroadband UV pulses with sub-10 fs duration and the implementation of a robust technique to fully characterize them and reconstruct their temporal profile; secondly, the generation of two phase-locked collinear UV pulses to be used as pump in 2DES. The work of this thesis is then organized in three main sections, concerning: (a) the generation of sub-10 fs broadband UV pulses by nonlinear upconversion with a broadband non-collinear OPA (NOPA); (b) the characterization of these UV pulses using two-dimensional spectral shearing interferometry (2DSI), of which we propose a robust implementation; (c) the realization of a birefringent interferometric device, able to generate two phase-locked collinear UV pulses. Very first results of 2DES in the UV range are finally presented as a validation of this work. Our UV pulses are generated by sum-frequency (SFG) between a broadband visible pulse produced by a NOPA and a narrowband pulse at 800 nm. Transform-limited (TL) UV pulses, tunable from 315 to 380 nm, are achieved by nonlinear phase transfer. To fully

characterize these pulses we apply two-dimensional spectral-shearing interferometry (2DSI), a technique based on nonlinear mixing, in our case difference-frequency generation (DFG), between the test pulse and two highly chirped replicas of an auxiliary pulse, known as ancillae. In 2DSI the delay of one of the ancillae is scanned over few optical cycles and the spectrum of the down-converted signal is recorded as a function of this delay, yielding a two-dimensional map which encodes the group delay of the test pulse. The technique is sensitive to the spectral shear of the ancillae, and any error on its calibration leads to uncertainty in the phase retrieval. For this reason we have implemented a robust method to generate the ancillae in 2DSI, based on spectral filtering in the Fourier plane of a 4-f zero-dispersion compressor, which allows the generation of two sheared and synchronized monochromatic fields (Fig.1a). With this optimized method we have measured 8.7 fs UV pulses (Fig.1b-c). The generation of two phase-locked collinear pulses in the UV range is not trivial to achieve: common interferometric devices are affected by the vibration of the optical components, and the required accuracy increases at shorter wavelengths. To solve this problem we have implemented the TWINS

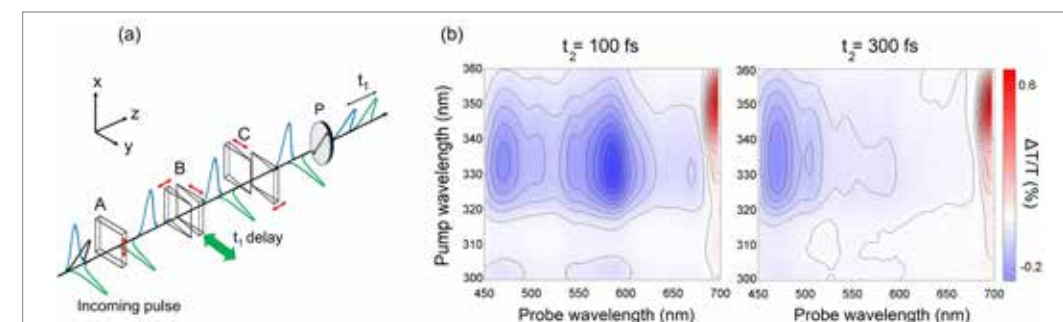
(Translating-Wedge-based Identical pulse eNcoding System) device, a simple and compact system which exploits birefringence to generate two phase-locked collinear pulses. It consists of a sequence of four birefringent wedges with different orientation of the optical axis, which creates two replicas of an input pulse. By changing their insertion into the beam path they can control with extreme accuracy (better than $\lambda/200$) the delay between the two generated pulses (Fig.2a). First, we have successfully applied TWINS in 2DES experiments in the visible and the IR ranges to study

the ultrafast interactions in a light harvesting complex. The reliability and stability of TWINS for 2DES in the visible range have suggested the possibility of extension of this technique to the UV range, where UV pulses are generated by nonlinear upconversion as described before. Actually, in order to avoid the considerable dispersion and the losses introduced by TWINS in the UV range, we have generated two pulse replicas in the visible range and made them interact in a SFG process with a quasi-monochromatic beam at 800 nm, ensuring upconversion

when scanning their relative delay. This way we have obtained two delayed upconverted replicas in the UV range to be used as pump in 2DES, enabling us to investigate dynamics and coupling mechanisms of many biomolecules absorbing in the 300-350 nm range. We have performed first measurements of UV-2DES to monitor femtosecond transient absorption in pyrene after excitation at 330 nm (Fig.2b). Future perspective is to perform UV-2DES spectroscopy in the 250-300 nm range, extremely promising for the study of photoprotection mechanisms in DNA.



1. Characterization of the UV pulses. (a) Ancillae generation in 2DSI configuration. A double-slit mask in the Fourier plane of the 4f pulse shaper selects two monochromatic ancillae, which interacts with the test pulse in a nonlinear process; the delay of one of the ancillae is scanned over few optical cycles (black arrow), recording the resulting spectrum with respect to this delay. (b) Characterization of a broadband UV pulse in the 310-380 nm range. Down-converted signal is recorded as a function of the delay of one of the ancillae. Black line: retrieved group delay of the pulse. (c) Retrieved temporal profile of the UV pulse. Measured duration is 8.7 fs, close to the TL value (black dashed line).



2. UV-2DES with TWINS. (a) Principle of TWINS device. Block A creates a constant “negative” delay between two perpendicularly polarized pulses. Wedges of block B scan the relative delay between the two pulses (green arrow). Wedges of block C correct for dispersion and front tilt. Polarizer P projects the two pulses to a common polarization direction. Red arrows indicate the direction of the optical axis of each plate. (b) First 2D spectra of pyrene in methanol showing evolution of transient absorption of the S2 \rightarrow S $_1$ (580 nm) and the S1 \rightarrow S $_0$ (465 nm) states after excitation at 330 nm, for two different values of pump-probe delay t_2 .

FEMTOSECOND LASER MICROMACHINING OF OPTOFLUIDIC GLASS CHIPS FOR BIOPHOTONIC APPLICATIONS

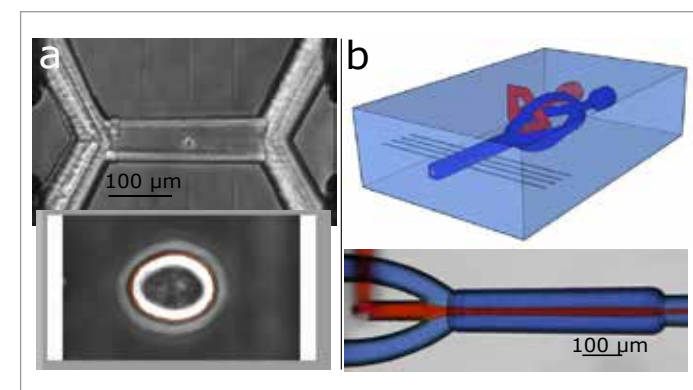
Petra Paiè - Supervisor: Roberto Osellame

During my PhD I have been working on the development of optofluidic devices fabricated by femtosecond laser micromachining. To explain this work it is necessary to introduce the concept of Lab On a Chip (LOC) systems, which are based on the idea to concentrate in a single and portable platform many functionalities used in chemical or biological laboratories. The core of these devices is often constituted by a net of microfluidic channels, whose dimensions are between tens and hundreds of micrometers. The synergy between these microfluidic devices and light is called optofluidic, and this is the field in which I mainly focused during my PhD. If on one side the fabrication techniques for microfluidic devices are well consolidated, it is not the same for the integration of the optical components in these platforms, due to the complexity of the fabrication processes and the difficult alignment of the components. A recently developed fabrication technique, femtosecond laser micromachining, overcome the current limitations, allowing to easily obtain compact optofluidic devices. Femtosecond laser pulses

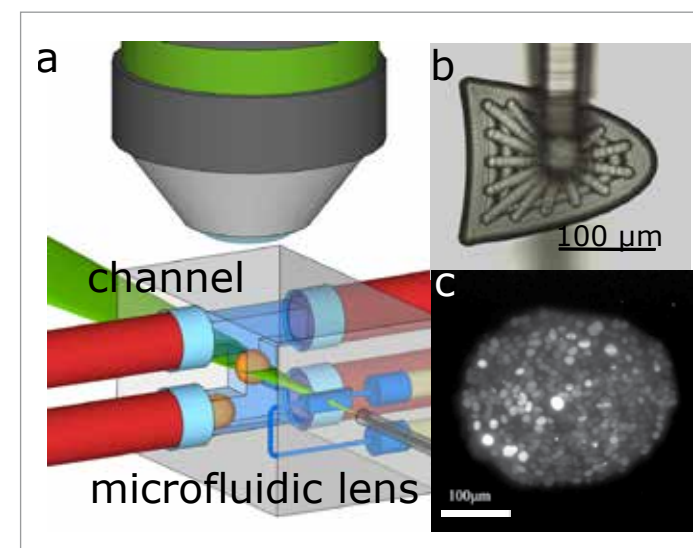
focused in a transparent material modifies permanently the substrate, due to non linear absorption processes that occur in the focal region. Thanks to this localization it is possible to have 3D pattern of modified areas, just translating the sample with respect to the laser beam. Depending on the irradiation parameters it is possible to obtain optical waveguides, structures capable to guide the light in a bulk substrate, and also microfluidic channel exposing the irradiated sample to an acid solution (HF). Basically with this technique it is possible to fabricate in the same substrate optical and fluidic circuits, perfectly aligned, with the desired 3D geometry. We have exploited this capability to develop two different devices, an optical stretcher (figure 1a) and a cell counter (figure 1b), where it is required to precisely control the position of waveguides with respect to the microchannel. The optical stretcher is a device that uses optical forces to analyze the deformability of single cells, using two waveguides that intercept orthogonally the microchannel, from the two opposite lateral sides of the channel. The device, placed under a microscope, permits to analyze the induced deformation

in real time. Since the chip presents two separate fluidic output, it is possible to physically separate the sample on the basis of these measures, just properly unbalancing the laser power coupled to the waveguides, so that the sample is pushed toward one of the two outputs. Regarding the cell counter instead this device again uses optical waveguides orthogonally facing the channel, but in this case the light is inserted from one side only, while from the other one the signal is collected, any variation in this signal indicate that a particle is flowing in the channel. It is important that all the sample elements flow one behind the other in between the two waveguides, so that the counting can be reliable. To obtain this feature we used hydrodynamic focusing, where lateral sheath flows of buffer are used to confine the sample in a micrometer-sized portion of the channel. In particular thanks to the 3D capability of the fabrication technique it has been possible to obtain with a really compact device a 3D confinement of the flow. This capability, which is not straightforward with other fabrication techniques, was necessary for the counting purpose, but can be easily

implement in many other applications which require a serial analysis of the sample. The other activity on which I worked is related to the fabrication of a compact device for integrated SPIM analysis, capable to overcome the low throughput of current approaches. SPIM, which stands for Selective Plane Illumination Microscopy, is a powerful microscopic technique, that allows 3D reconstruction of biological samples, through optical sectioning. It relies on the illumination of the sample performed with a sheet of light, which can be obtained focusing the beam in one direction only using a cylindrical lens. The translation of the sample is necessary to perform the optical sectioning and the 3D reconstruction. Low photo toxicity, high signal to noise ratio and fast acquisition are typical of this method. Nevertheless the main drawback of this technique is the long mounting time which, lasting several minutes, prevents the use of SPIM for the analysis of big population of sample. The device we wanted to fabricate is a compact platform capable to perform SPIM at high throughput (figure 2a). The sheet of light is obtained with an integrated microfluidic cylindrical lens (a microchannel filled with a refractive index oil). The shape of this lens has been optimized to reduce the impact of spherical aberrations (figure 2b), which allows to have a thinner light sheet and consequently an higher lateral resolution. The fluidic circuits delivers the sample through the



1. Fig 1a top: microscope image of the optical stretcher, bottom: detail of a stretched cell. Fig 1b top: schematic design of the cell counter, bottom: microscope image of hydrodynamic focusing characterization: the sample (in red) is confined using lateral fluids (in blue).



2. on the left, an image of a typical top-gated phosphorene device; on the right, the best on/off ratio obtained and a plot showing ambipolar behavior in one of the samples.

light sheet, so that while flowing it is sectioned by the excitation light. This device so fabricated is really compact and thanks to its portability can be easily mounted on a standard microscope. The chip has been successfully tested

with cells spheroids (figure 2c), which are aggregate of cells of about 300 μm, validating not only the quality of the images but also the high throughput, measuring up to 30 spheroids per minute.

TITANIUM DIOXIDE HIERARCHICAL NANOSTRUCTURES FOR PHOTONIC APPLICATIONS

Luca Passoni - Supervisor: Dr. Fabio Di Fonzo

Nanotechnology was first envisioned by *Richard P. Feynman* as a field in which the technical capability of manipulating things on a small scale, could have paved the way to an enormous number of possible applications. Today, after decades of research, materials with nanometric features (nanomaterials) have given access to the understanding and to the control of a wide range of phenomena. Nanomaterials, differently from bulk materials, comprise building blocks having often the characteristic size of the physico-chemical phenomenon that is interacting. For example photovoltaic materials work thanks to their active structure being as thick as the incident light penetration depth and the electron diffusion length, photonic crystal modulate light flow thanks to a dielectric constant spatial modulation in the order of a quarter of the wavelength, or superhydrophobic structures have reduced wettability as they can lower their surface free energy at the interface with the liquid at a molecular scale. In order to obtain nanomaterials, several fabrication techniques were implemented either following a top-down or a bottom-up approach. Among many techniques falling in the former approach, anodic etching have been widely used

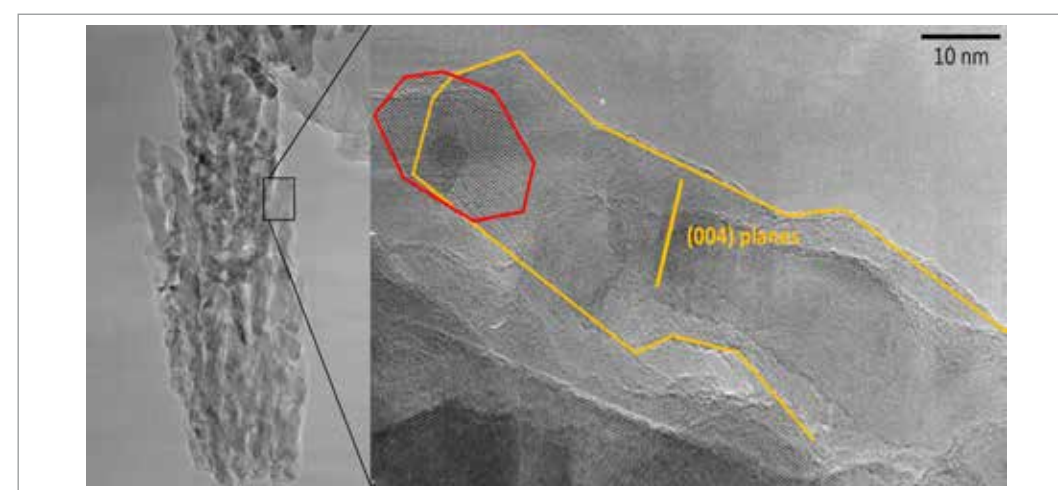
to selectively etch materials leaving elongated structures called nanotubes and lithography, as well as, femtosecond laser ablation, can obtain complex micro patterning by precisely and selectively removing materials while leaving untouched other by chemical reaction and by physical ablation respectively. Despite the industry still relies heavily on these techniques for several applications (e.g. microelectronic), top-down approach has a major drawback in the fact that it is intrinsically bound to a template material from which it must extract the desired micro or nanostructure. The fabrication and the properties of the template in turn limit the possibilities of this techniques; anodic etching can only be applied to conductive materials, lithography to reactive layers and femtosecond laser ablation to a specific set of materials. These limitations are not present in bottom-up fabrication methods. The latter's are additive manufacturing techniques rather than subtractive and relate those mentioned before in a similar fashion as 3D printing does with fabrication methods of standard objects. Among bottom-up approaches physical vapour deposition (e.g. pulsed laser deposition) comprises a set of techniques that exploit evaporation to transfer a material

in the gas-phase from a source to a target. In this context the *Ph.D. thesis* entitled "*Titanium dioxide hierarchical nanostructures for photonic applications*" aims to explore the potentiality of pulsed laser deposition (PLD) in material nanostructuring. Titanium dioxide (TiO_2) is a fascinating large band-gap semiconductor material. TiO_2 is abundant in nature, biocompatibility and possesses outstanding properties such as efficient electron transport, transparency, photocatalytic activity. Pulsed laser deposition is used to tailor its structural properties. By changing process parameters it is possible to tune the kinetic of recondensation of the laser vaporized titanium dioxide. In particular it is shown how the clusters ejected from the source materials upon laser ablation reacts to the oxygen partial pressure within the deposition chamber and how this can eventually be used to control the kinetic of cluster reorganization into different nanostructures. While in low oxygen conditions, highly energetic species are forming compact films, high oxygen pressure are employed to induce cluster scattering and to control the consequent formation of more complex hierarchical nanostructures. Nanometric

features attached to branches departing from a main vertical trunk give to these structures high specific surface that increase with porosity at higher deposition pressure. Higher surface area per unit volume (roughness factor) is found in dense hierarchical materials, that are therefore of interest for all those application where interfacial phenomena are crucial. Besides causing high roughness factor, material density is responsible for a particular crystallization. Thermal energy provided to dense hierarchical structures during thermal annealing is shown to start an energy minimization process leading to the formation of crystalline structures as long as hundreds of nanometers (hyperbranching). In turn crystallization process parameters are used to further tailor the nanostructures. Thermal annealing does not only change nanometric feature size but, dependently

on initial morphology, it strongly effects the pores size distribution. The overall pore volume is decreased as an effect of thermally induced Oswald ripening. In fact nanocrystalline average grain size increases driving a suppression of nanometric pores that increases the average pores size and reduce the overall volume. Exploiting the morphology control, hierarchical one dimensional photonic crystals are obtained by periodically modulating the nano-structural effective refractive index through the modulation of the density. Alternatively if the porosity is left constant hierarchical nanostructures grow with an inverse conical envelop with lateral dimension of few hundreds of nanometers and they act as an array of Mie scattering elements forming a hazy film. Hyperbranched nanostructures were employed as photoanodes in standard liquid and solid state dye sensitized solar cells. Scattering

hyperbranched nanostructures are shown to improve photovoltaic performances thanks to an enhanced optical density and more efficient charge extraction. Similar structures upon effective refractive index modulation form hierarchical one dimensional photonic crystal and are used as photoanodes for structurally coloured solar cells. Hierarchical photonic crystals are also envisioned in light of possible applications in the field of active matrix displays, sensing devices and optical materials for telecommunication. Eventually it is shown how the study and the control over hierarchical nanostructures morphology had a fall-out in the wettability control. Transparent self-cleaning surfaces are studied as a possible overlayer for those opto-electronic devices operating in outdoor environments such as photovoltaic solar cells.



1. Transmission electron microscope images showing the hyperbranched crystallinity of annealed samples of TiO_2

LIGHT HARVESTING AND PHOTOPROTECTION IN NATURAL AND ARTIFICIAL SYSTEMS

Daniele Viola - Supervisor: Prof. Giulio Nicola Cerullo

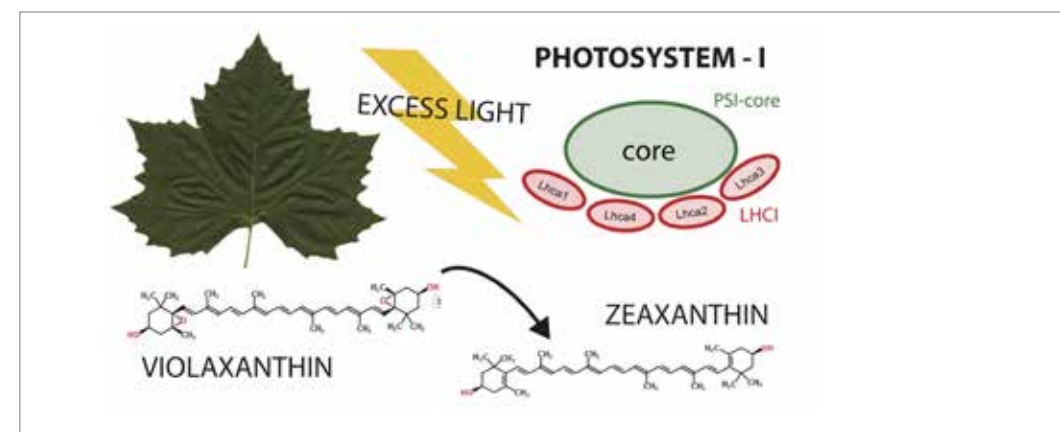
We rely on oil, gas and coal for the great majority of our current energy needs, furthermore this energy demand is expected to grow by 50% over the next 20 years, and at this rate of demand growth we have enough supply for 30 years. The almost unlimited supply potential of renewable energy sources, such as solar energy, can be the solution not to run out of it.

Solar energy, which is efficiently harvested by photosynthetic systems such as plants, algae and bacteria, can be used in two ways for energy production: exploiting directly the photosynthetic systems (which are not used for food or feed) in order to create biomass or biofuels, or directly generating electrical currents from photovoltaic solar energy conversion.

This thesis uses ultrafast optical spectroscopy to investigate the primary photoinduced processes in different natural and artificial light-harvesting systems. Both in plants and in bacteria the first step of photosynthesis is the light harvesting: a photon is absorbed generating an excited electron by the pigments (chlorophylls and carotenoids) of the outer antenna complexes, which will transfer this energy through a sequence of steps

into the reaction center, where it will be used to create adenosine triphosphate (ATP). In this process, carotenoids play a key role: they are pigments that extend the light absorption in the blue-green region (where chlorophylls poorly absorb) and at the same time they have a photo-protective role. They have been widely studied as they are involved in the primary light harvesting processes, and their ultrafast internal conversion and energy transfer are deeply connected to the process efficiency. These studies discovered the existence of a new dark electronic state, named S^* whose nature is still under debate. We investigated its origin by performing a series of pump-probe experiments with sub-20 fs time resolution on the carotenoid spirilloxanthin changing the sample temperature. After excitation an ultrafast internal conversion occurs: within 200 fs the system decay from S_2 to the lower levels S_1 and S^* , which in turn relax to the ground state on a picosecond time scale. Cooling the system down to 77 K, a systematic decrease of S^*/S_1 ratio is shown. Such a result can be explained with two thermally populated ground state isomers, where the higher state generates S^* that can be frozen out by cooling.

The other role of carotenoids is the photo-protection from excess illumination; to this regard we studied zeaxanthin, a carotenoid produced from preexisting violaxanthin upon excess light conditions. Zeaxanthin binding to the photosystem II (PSII) antenna system has been widely investigated and shown to help in excess chlorophyll excited state dissipation and as oxygen radicals scavenger. However its presence in the photosystem I (PSI) antenna has not been clarified yet. For this reason we investigated the role of zeaxanthin performing time-resolved fluorescence measurements on preparations isolated from wild-type PSI (with violaxanthin) and those from a mutant in which violaxanthin is replaced by zeaxanthin. We showed that zeaxanthin has a dissipative role in PSI too, similar to the behavior in PSII. Understanding the dissipation processes in photosynthetic systems is practically important, as a big limitation in achieving high photosynthetic efficiency in biomass production is the fact that the sunlight often exceeds the photosynthetic capacity of cells and the excess of light energy is predominantly dissipated as heat, decreasing the light use efficiency of the culture.



1. Drawing showing how in excess light condition, violaxanthin-zeaxanthin cycling occurs in PSI, in order to photoprotect it.

In photovoltaic systems the aim is to generate directly electrical current. In contrast with inorganic semiconductors such as silicon, polymers provide several advantages, such as low cost and flexibility. However, the generation of free charges in polymers is comparatively inefficient, since the absorbed light results in the creation of tightly bound electron-hole pairs, known as excitons. To enable their use in photovoltaic solar cells, polymers are usually mixed with another material that will extract the electrons to form a heterojunction: the donor-acceptor junction provides the necessary force to dissociate and spatially separate the excitons. Photogeneration of charged states has also been observed in neat films of conjugated polymers. These charged states can be defined as polaron pairs (PPs); in a PP, the electron and hole are more separated in space compared to an exciton. Usually the PP generation yield is very small, but nevertheless it could

be relevant in neat polymers: in heterojunctions used in polymer solar cell there are domains of a few tens nm size, therefore it's important to understand all the contribution to the free charges that lead to the direct current power. For this reason we studied the charge photogeneration yield in neat films of the PCPDTBT polymer monitoring the ultrafast photoinduced absorption of PPs in comparison to that of excitons. We showed that in aggregated polymers the charge generation yield is quite high and therefore it should be taken in account when optimizing film morphologies for organic photovoltaic devices.

The last part of my PhD work focused on the photophysics of perovskites, which are very inexpensive hybrid organic-inorganic materials used to replace the expensive crystalline silicon solar cells. These materials created much excitement as they allowed power conversion efficiency higher than 20%. The

problem is that the performances of photovoltaic devices are dependent on poorly reproducible preparation conditions. It is not clear yet how the perovskite structure affects its properties; in previous characterizations of their optical and physical properties, macroscopic portions of the material were analyzed and therefore the mesoscale material diversity was averaged out. For this reason we developed a system that enabled us to perform pump-probe microscopy and we used it to understand the behavior of micrometer-size perovskite crystals: the results of the pump-probe microscopy, together with Raman microscopy suggested that perovskite optoelectronic properties, and thus their photovoltaic efficiency, strongly depend on local lattice distortions.